https://ntrs.nasa.gov/search.jsp?R=19780005919 2020-03-22T05:33:16+00:00Z

General Disclaimer

One or more of the Following Statements may affect this Document

- This document has been reproduced from the best copy furnished by the organizational source. It is being released in the interest of making available as much information as possible.

- This document may contain data, which exceeds the sheet parameters. It was furnished in this condition by the organizational source and is the best copy available.

- This document may contain tone-on-tone or color graphs, charts and/or pictures, which have been reproduced in black and white.

- This document is paginated as submitted by the original source.

- Portions of this document are not fully legible due to the historical nature of some of the material. However, it is the best reproduction available from the original submission.

Produced by the NASA Center for Aerospace Information (CASI)

INTERACTIONS OF SATELLITE-SPEED HELIUM ATOMS WITH SATELLITE SURFACES

III: DRAG COEFFICIENTS FROM SPATIAL AND ENERGY DISTRIBUTIONS OF REFLECTED HELIUM ATOMS

(NASA-CR-155340) INTERACTIONS OF SATELLITE-SPEED HELIUM ATOMS WITH SATELLITE SURFACES. 3: DRAG COEFFICIENTS FROM SPATIAL AND ENERGY DISTRIBUTIONS OF REFLECTED HELIUM ATOMS (California Univ.) G3/72 55216

N78-13862

Unclas

Prepared by:

P. K. Sharma, Postdoctoral Scholar
E. L. Knuth, Professor

Chemical, Nuclear, and Thermal Engineering Department
School of Engineering and Applied Science
University of California, Los Angeles
Los Angeles, CA 90024

for

NASA Langley Research Center
Hampton, VA 23365

under

Grant NGR-05-007-416

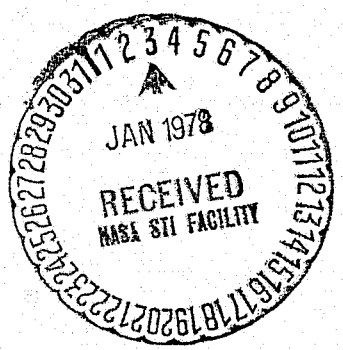

December 1977

CHAPTER I

INTRODUCTION

The studies reported here were part of a long-range program conducted in the UCLA Molecular-Beam Laboratory with the objective of adding to the available knowledge concerning energy and momentum transfers between satellites and upper-atmosphere gases. Important applications of such knowledge include (a) estimating the lifetimes of satellites for given atmospheric models and (b) extracting upper-atmosphere densities from satellite-drag data.

The aerodynamic drag of a satellite is predicted sometimes using a model in which the energy accommodation between the incident molecules and the satellite surface is complete and the reflected molecules are scattered diffusely (with a cosine scattering distribution). However, deviations from this idealized model could yield significantly different satellite drags. Hence, specific objectives of the present studies included (a) measurements of energy accommodation as a function of incidence angle and scattering direction, (b) measurements of scattering distribution as a function of incidence angle, and (c) calculation of the drag coefficient from the forementioned measurements.

The studies of the interactions of satellite-speed helium atoms with satellite-type surfaces were initiated by Dr. S. M. Liu. Spatial distributions of helium atoms reflected from several satellite-type surfaces are summarized in Ref. 1; energy distributions of helium atoms reflected from a 6061 T-6 aluminum surface are summarized in Ref. 2. In the present report, spatial and energy distributions of helium atoms scattered from an anodized 1235-0 aluminum surface (also tangential and normal momentum

accommodation coefficients calculated from these distributions) are reported. Included are (a) a procedure for calculating drag coefficients from measured values of spatial and energy distributions and (b) the drag coefficient calculated for a 6061 T-6 aluminum sphere from the data reported in Refs. 1 and 2. The drag coefficient for an anodized aluminum sphere will be reported in a later publication.

CHAPTER II

EXPERIMENTAL METHODS

The present study was carried out in the UCLA Molecular-Beam Laboratory using the molecular-beam system shown schematically in Fig. 1. The satellite-speed helium beam was generated using the arc-heated supersonic beam source developed by Young[3] and passing the central portion of the arc-heated jet through a skimmer and two collimating orifices. The resulting beam was characterized by a multi-disk velocity selector whose orientation and angular speed were adjusted to yield a 7000 m/sec beam.

The detection system (Fig. 1) facilitated measurements of the three-dimensional scattering distributions and the energy distributions of the scattered atoms. The system included a target positioning mechanism, a detector rotating mechanism and a mass spectrometer and/or a retarding-field energy analyzer. These components are described in Ref. 2.

Spatial-Distribution Measurements

Spatial distributions of a helium beam reflected from an anodized aluminum surface were measured essentially as described in Ref. 2. The main difference in the present measurements was that the distance between the surface and the entrance orifice of the ioniser was reduced to one inch (from the two inches used previously) in order to increase the signal intensity. A block diagram of the electronic system for the mass spectrometer and the multi-disk velocity selector is shown in Fig. 2.

Energy-Distribution Measurements

The energy distributions were measured using the retarding-field energy analyzer described in Ref. 2 and the detection system (a slight modification of the one described in Ref. 2) shown schematically in Fig. 3. The energy spectrum of the reflected atoms at a given scattering

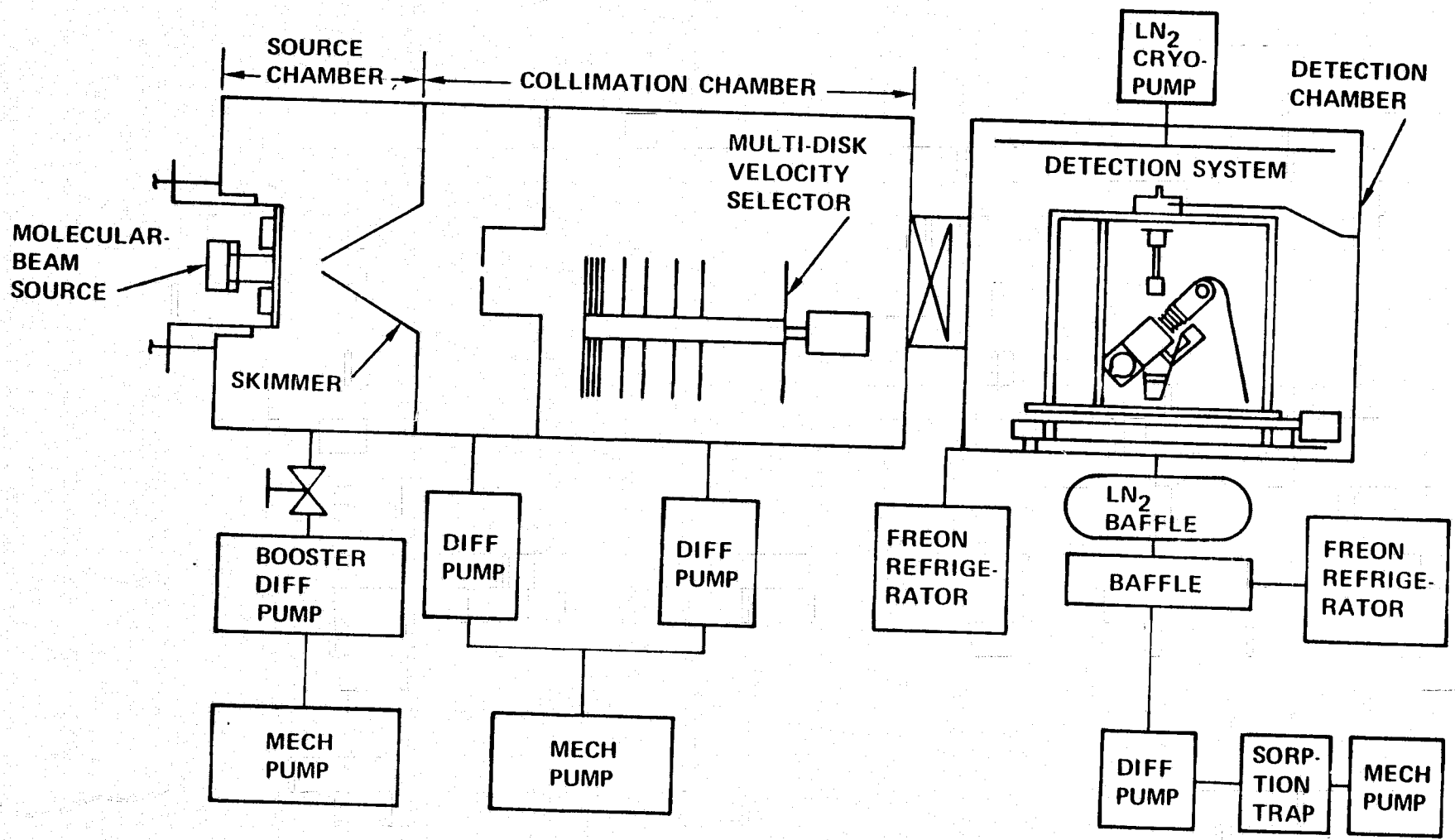

Figure 1. Schematic Diagram of the Molecular Beam System.

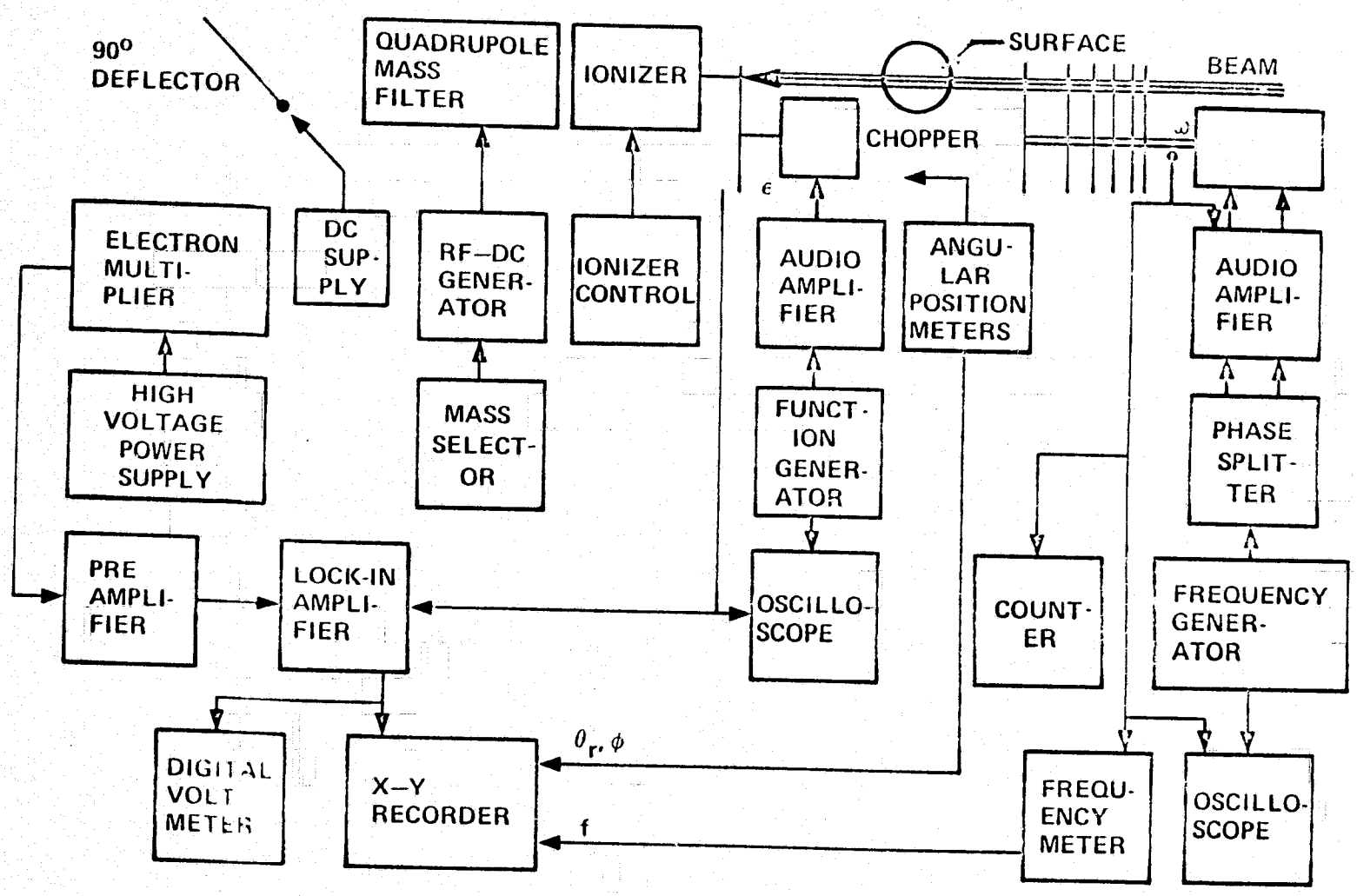

Figure 2. Block Diagram of the Electronic System of the Mass Spectrometer and the Multi-Disk Velocity Selector.

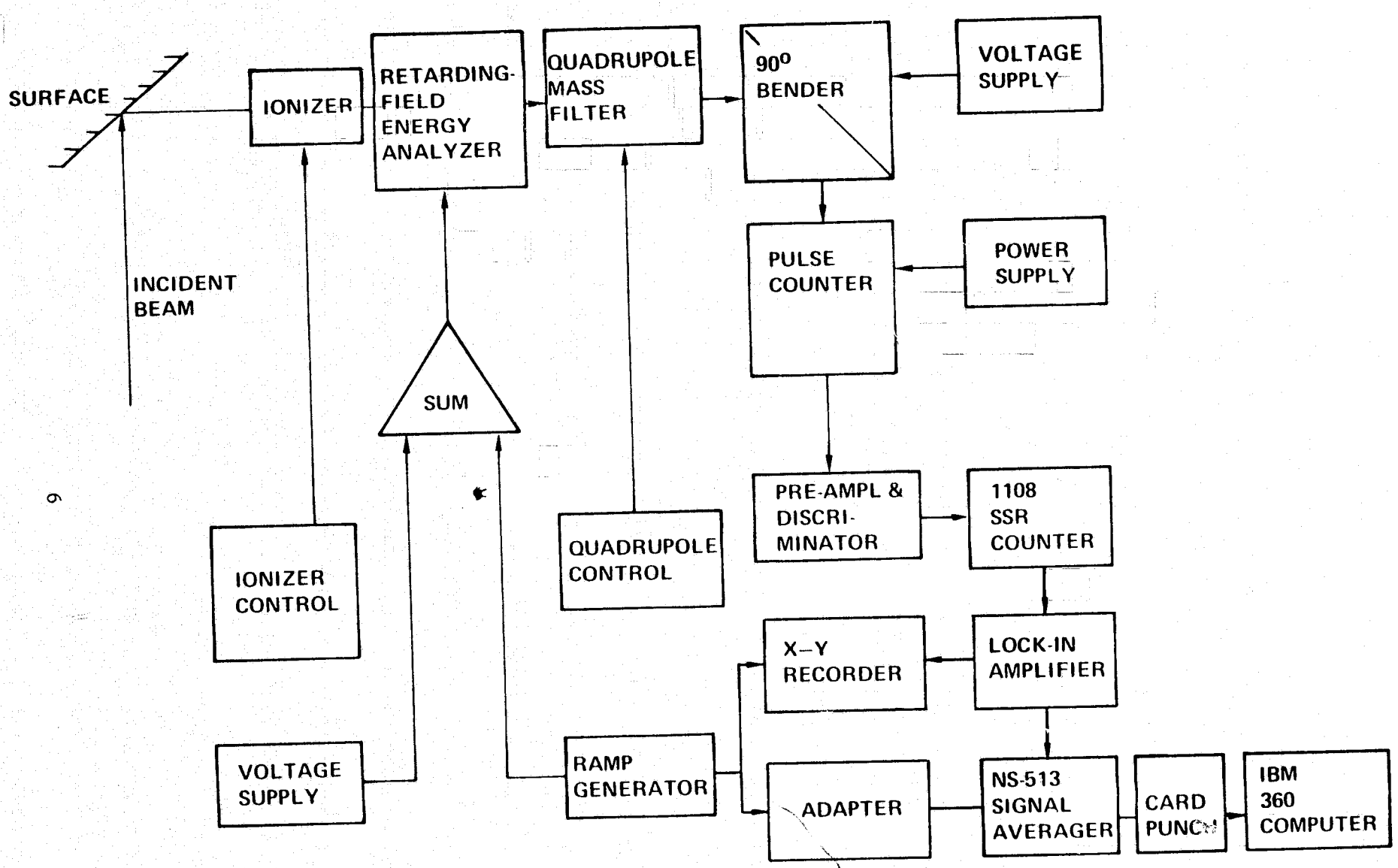

Figure 3. Block Diagram of the Detection System.

angle was obtained by measuring the reflected-beam density as a function of the retarding potential. In the arrangement described in Ref. 2, the incident beam was not modulated so that the measurement included contributions from both the reflected beam and the background; the background contribution was determined in a separate measurement by intercepting the incident beam by a flag located inside the detection chamber. In the arrangement used here, (a) the beam entering the detection chamber is modulated by a chopper rotating at 10 cps before it impinges on the target surface, (b) the signal from the SSR counter is fed to an Ithaco Dynatrac 391A lock-in amplifier and (c) the output of the lock-in amplifier represents the contribution from the beam alone since the background contribution is subtracted automatically.

Surface Preparation

The target used in the present studies was cut from a 0.005-in.-thick anodized 1235-0 aluminum foil provided by personnel at the NASA Langley Research Center. The surface was cleaned with acetone prior to installation on the target holder.

CHAPTER III

EXPERIMENTAL RESULTS

Spatial Distributions

Spatial distributions measured for a satellite-speed (7000 m/sec) helium beam scattered from an anodized 1235-0 aluminum surface for six different incidence angles (0°, 15°, 30°, 45°, 60°, and 75° from the surface normal) are shown in Figures 4-9. In these figures, the center of the polar diagram corresponds to the point of impingement. The incident beam impinges on the test surface (which coincides with the surface of the page) from the bottom of the diagram with the given incidence angle measured from the surface normal. The upper ($\theta_r > 0$) and lower ($\theta_r < 0$) halves of the diagram represent the forward-scattering and backward-scattering regions respectively. The dashed lines at constant value of θ_r indicate detector paths from $\phi = 0°$ to $\phi = 90°$, where ϕ denotes the out-of-plane scattering angle.

These plots exhibit trends similar to those found for a 6061 T-6 aluminum surface [2]. Of special significance (for both the present surface and the 6061 T-6 surface) is the backscattering, which becomes more prominent as the incidence angle increases toward the surface tangent (i.e., for large values of θ_i). Such backscattering yields relatively high drag coefficients.

Energy-Accommodation Coefficients

Measurements of energy distributions of satellite-speed helium atoms scattered from an anodized aluminum surface were made for six different incidence angles (θ_i = 0°, 15°, 30°, 45°, 60° and 75° from the surface normal). For each incidence angle, distributions were measured at approximately forty scattering positions. These scattering positions were chosen

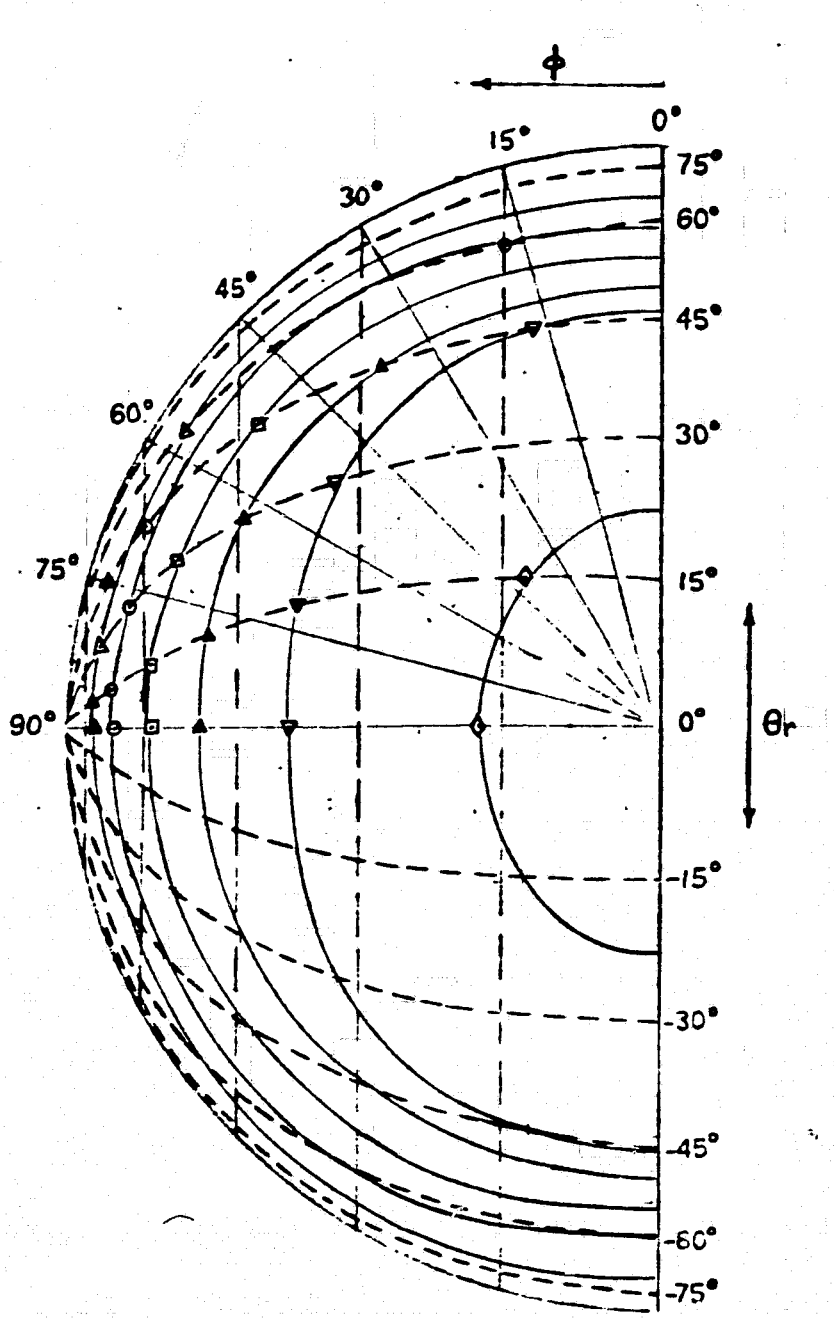

FIG. 4. POLAR PLOT OF SCATTERED-BEAM DENSITY DISTRIBUTION FOR 7000 m/sec HELIUM BEAM SCATTERED FROM ANODIZED ALUMINUM SURFACE AT 0° INCIDENCE ANGLE.

ORIGINAL PAGE IS
OF POOR QUALITY

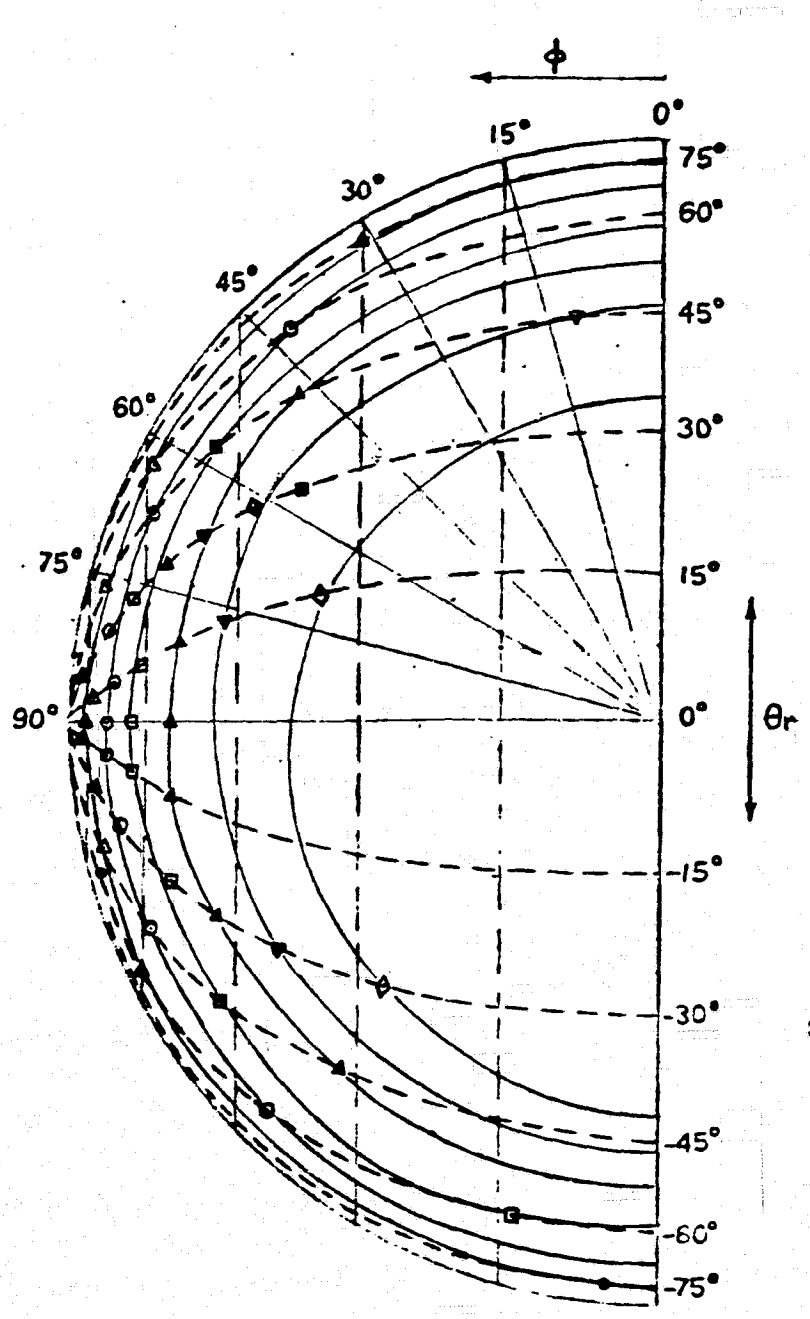

FIG.5. POLAR PLOT OF SCATTERED-BEAM DENSITY DISTRIBUTION FOR 7000 m/sec HELIUM BEAM SCATTERED FROM ANODIZED ALUMINUM SURFACE AT 15° INCIDENCE ANGLE.

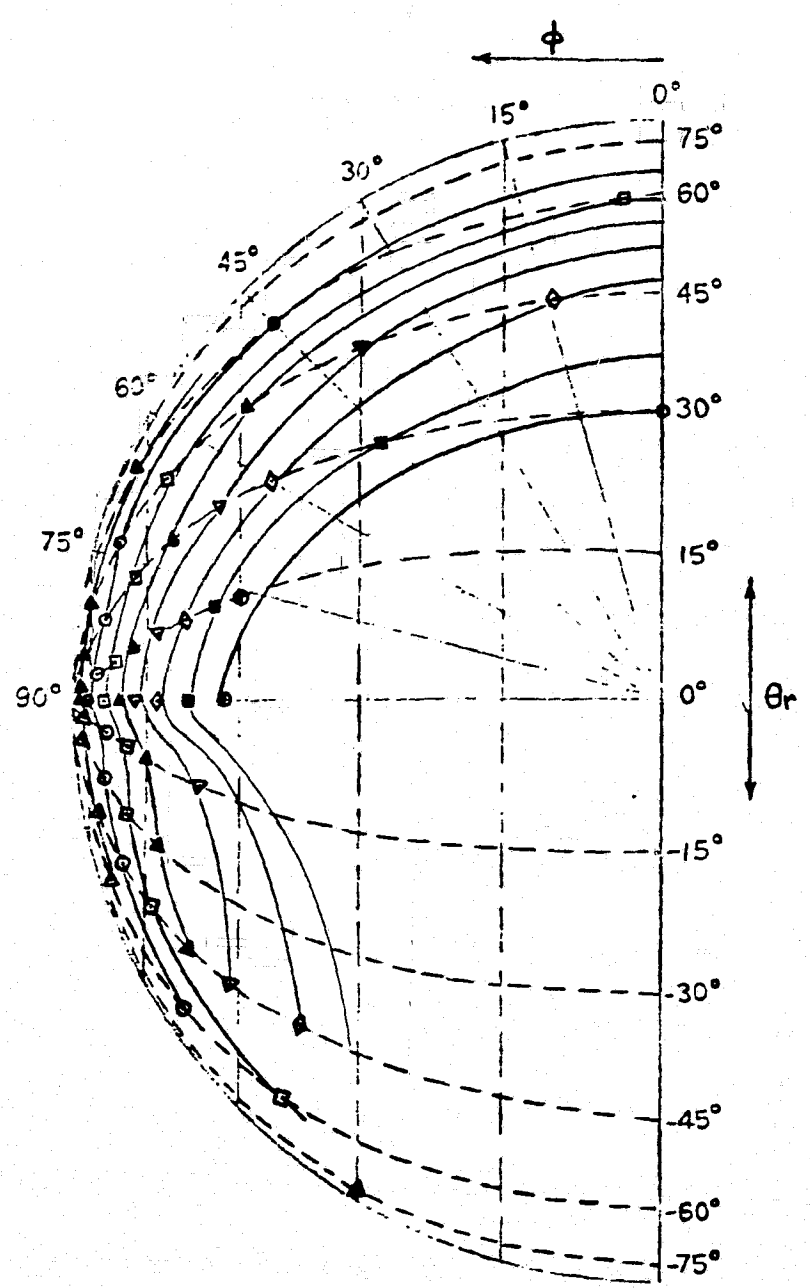

SYMBOL	DENSITY
△	1·5
○	2.0
□	2·5
▲	3·0
▽	3·5
◇	4·0
■	4·5
●	5.0

FIG. 6. POLAR PLOT OF SCATTERED-BEAM DENSITY DISTRIBUTION FOR 7000 m/sec HELIUM BEAM SCATTERED FROM ANODIZED Al SURFACE AT 30° INCIDENCE ANGLE.

ORIGINAL PAGE IS
OF POOR QUALITY

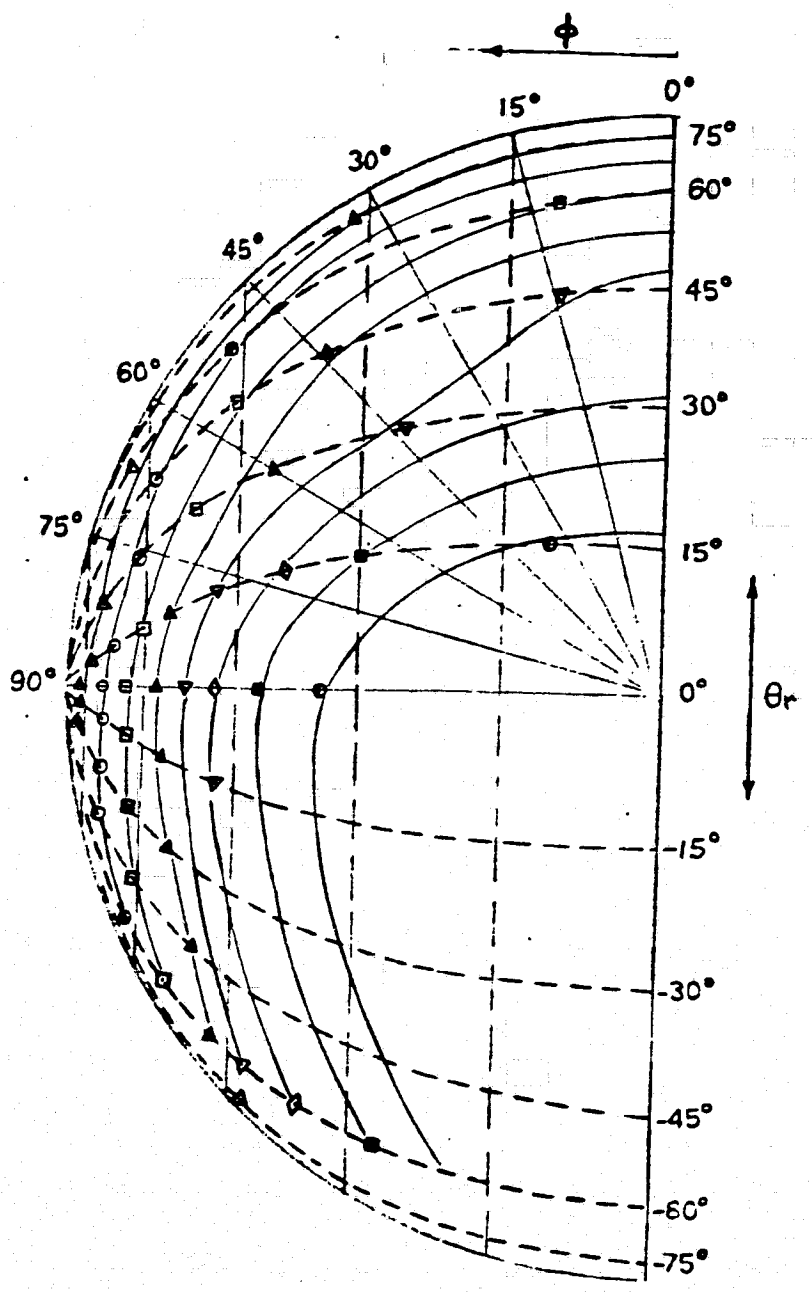

SYMBOL	DENSITY
●	1·0
△	1·5
○	2.0
□	2·5
▲	3.0
▽	3·5
◇	4·0
■	4.5
◉	5.0

FIG.7. POLAR PLOT OF SCATTERED-BEAM DENSITY DISTRIBUTION FOR 7000 m/sec HELIUM BEAM SCATTERED FROM ANODIZED Al SURFACE AT 45° INCIDENCE ANGLE.

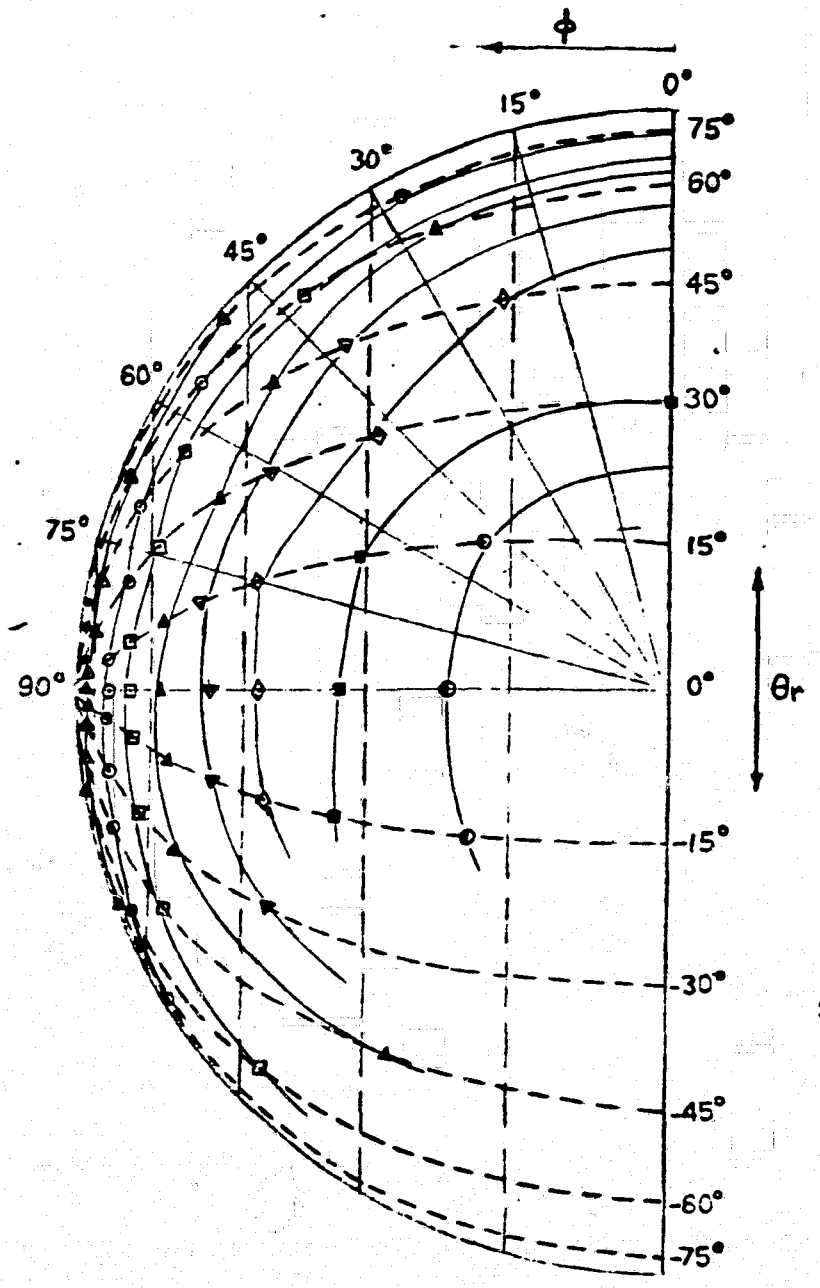

FIG. 8. POLAR PLOT OF SCATTERED-BEAM DENSITY DISTRIBUTION FOR 7000 m/sec HELIUM BEAM SCATTERED FROM ANODIZED Al SURFACE AT 60° INCIDENCE ANGLE.

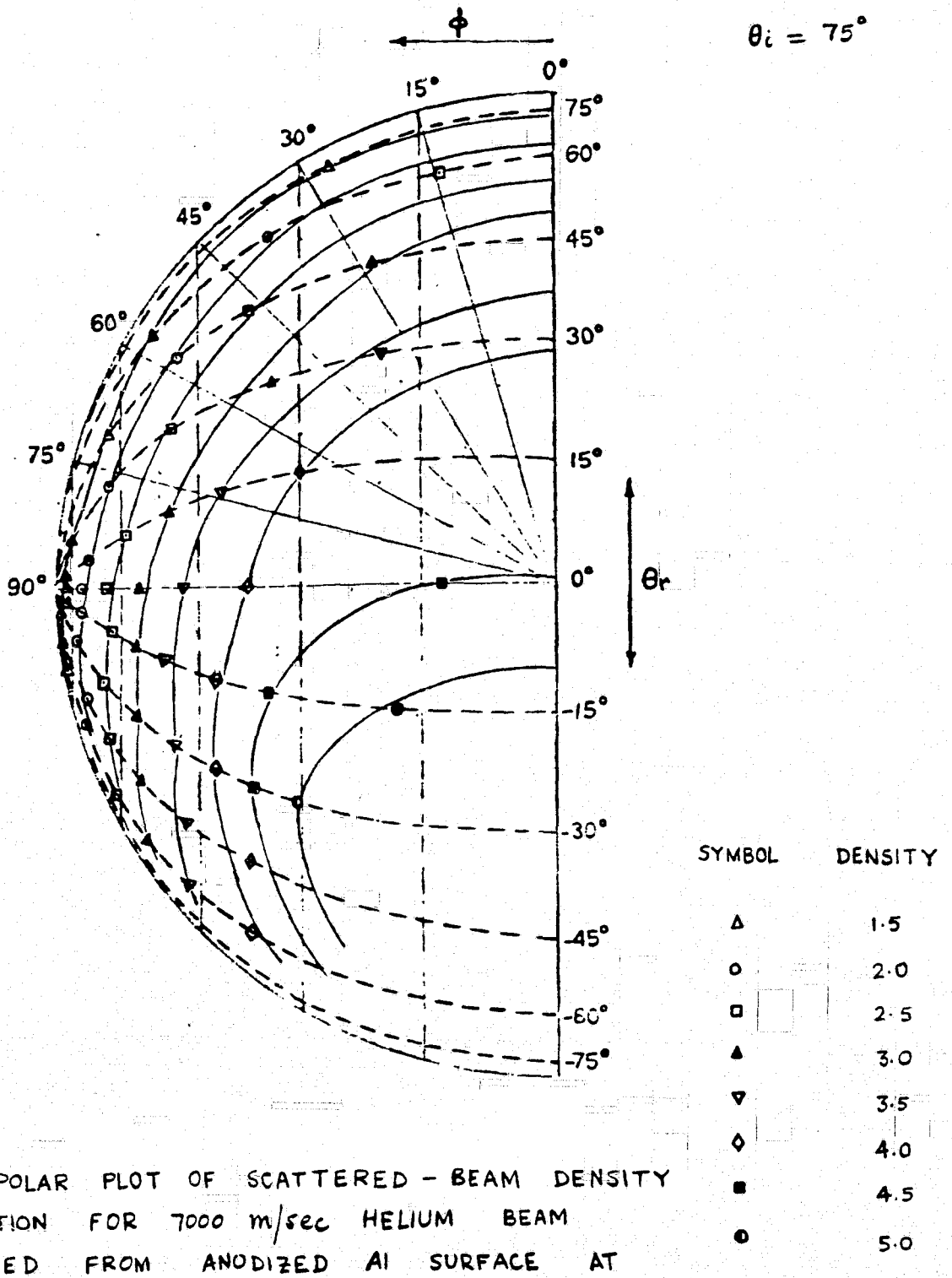

FIG.9. POLAR PLOT OF SCATTERED - BEAM DENSITY DISTRIBUTION FOR 7000 m/sec HELIUM BEAM SCATTERED FROM ANODIZED Al SURFACE AT 75° INCIDENCE ANGLE.

from eleven in-plane scattering angles (θ_r = ± 75°, ± 60°, ± 45°, ± 30°, ± 15° and 0°) and six out-of-plane scattering angles (ϕ = 0°, 15°, 30°, 45°, 60° and 75°). Measurements were not possible within a solid angle around the incident beam (due to interference between the detector and the incident beam at these scattering positions) and for some glancing scattering angles (due to weak signal-to-noise ratios).

The data obtained for the net helium beam as well as for the background helium was recorded both on chart-recorder paper as well as on computer cards. It was analyzed using the procedure described in Ref. 2. The resulting differential energy accommodation coefficients $(AC)_E$ (θ_i, θ_r, ϕ) obtained at all possible scattering angles are given in Tables I-VI.

The differential energy accommodation coefficients obtained show some fluctuations, due apparently to the weak signal-to-noise ratio which results from the relatively diffuse scattering.

TABLE-I . THE DIFFERENTIAL ENERGY ACCOMMODATION COEFFICIENTS FOR 7000 m/sec HELIUM BEAM SCATTERED FROM ANODIZED ALUMINUM SURFACE AT 0° INCIDENCE ANGLE.

ϕ \ θ_r	-75°	-60°	-45°	-30°	-15°	0°	15°	30°	45°	60°	75°
0°		57	85						85	57	
15°		47	60						60	47	
30°		42	58	43				43	58	42	
45°		44	62	70	67	57	67	70	62	44	
60°			55	80	60	50	60	80	55		
75°											

TABLE - II . THE DIFFERENTIAL ENERGY ACCOMMODATION COEFFICIENTS FOR 7000 m/sec HELIUM BEAM SCATTERED FROM ANODIZED ALUMINUM SURFACE AT 15° INCIDENCE ANGLE.

ϕ \ θ_r	-75°	-60°	-45°	-30°	-15°	0°	15°	30°	45°	60°	75°
0°		65						43	51	47	
15°		58						30	42	44	
30°		62	53				44	49	43	38	
45°		53	52	54	59	48	40	51	34		
60°		47	46	48	45	43	34	28	25		
75°											

TABLE - III . THE DIFFERENTIAL ENERGY ACCOMMODATION COEFFICIENTS FOR 7000 m/sec HELIUM BEAM SCATTERED FROM ANODIZED ALUMINUM SURFACE AT 30° INCIDENCE ANGLE.

ϕ \ θ_r	-75°	-60°	-45°	-30°	-15°	0°	15°	30°	45°	60°	75°
0°		61				30	53	52	44	47	
15°		68				70	62	49	56	53	
30°		74				80	66	63	54	51	
45°		65	69	72	80	75	66	61	58		
60°			57	58	70	64	51	46			
75°											

TABLE - IV . THE DIFFERENTIAL ENERGY ACCOMMODATION COEFFICIENTS FOR 7000 m/sec HELIUM BEAM SCATTERED FROM ANODIZED ALUMINUM SURFACE AT 45° INCIDENCE ANGLE.

ϕ \ θ_r	-75°	-60°	-45°	-30°	-15°	0°	15°	30°	45°	60°	75°
0°						59	61	71	57	39	
15°						67	53	66	51	32	
30°					57	63	50	43	74	44	
45°		72	68	75	52	58	62	64	62		
60°			63	56	68	51	56	52			
75°											

TABLE - V . THE DIFFERENTIAL ENERGY ACCOMMODATION COEFFICIENTS FOR 7000 m/sec HELIUM BEAM SCATTERED FROM ANODIZED ALUMINUM SURFACE AT 60° INCIDENCE ANGLE.

ϕ \ θ_r	-75°	-60°	-45°	-30°	-15°	0°	15°	30°	45°	60°	75°
0°					51	59	66	69	65	80	
15°					58	53	57	58	64	74	
30°				52	54	49	38	40	56	50	
45°		64	55	49	42	38	25	44	62		
60°		33	47	48	44	40	31	20			
75°											

TABLE – VI. THE DIFFERENTIAL ENERGY ACCOMMODATION COEFFICIENTS FOR 7000 m/sec HELIUM BEAM SCATTERED FROM ANODIZED ALUMINUM SURFACE AT 75° INCIDENCE ANGLE.

ϕ \ θ_r	-75°	-60°	-45°	-30°	-15°	0°	15°	30°	45°	60°	75°
0°				40	62	55	58	44			
15°				72	85	67	49	51			
30°				64	77	61	54				
45°					71						
60°											
75°											

CHAPTER IV

EVALUATION OF DRAG COEFFICIENT FOR THE 6061-T6 ALUMINUM SURFACE

This chapter summarizes the procedures used to deduce a drag coefficient for spheres from measured differential energy-accommodation coefficients, and gives the value deduced for a 6061-T6 aluminum sphere using the measurements made by Liu[2].

Extrapolation of Scattering-Distribution and Energy-Accommodation Measurements

Recall that scattering and energy distributions could not be measured in a significant portion of the back-scattering region due to interference of the detector with the beam. In addition, energy distributions could not be measured for large values of the scattering angle, θ_r, and the azimuthal angle, ϕ, due to the weakness of the signal at these angles. Hence the following method was devised to extrapolate the measurements to regions where measured values are not available.

If, for a given value of θ_i, one plots the scattering distributions measured in two orthogonal planes (one plane defined by a constant value of ϕ, the other by a constant value of θ_r), then the scattered-beam density at the intersection of these two planes must be common to both planes. Thus, the density at a particular point could be determined, if the values in its vicinity in two orthogonal planes passing through this point were known, by extrapolating in both planes to a common value at this point. The estimated value at this point could be used now in the estimation of the density at a new point in its vicinity.

This procedure was used to fill in the gaps in Tables III-1 - III-6 of Ref. 2, where measured values of density and energy accommodation

coefficients are reported. Both the measured and extrapolated results are given in Tables VII - XII of the present report.

Differential Normal and Tangential Momentum Accommodation Coefficients

Differential momentum accommodation coefficients may be defined as

$$\alpha_{NM} = \frac{(\vec{p}_i - \vec{p}_r)_N}{(\vec{p}_i - \vec{p}_w)_N} = \frac{(\vec{v}_i - \vec{v}_r)_N}{(\vec{v}_i - \vec{v}_w)_N}$$

$$\alpha_{TM} = \frac{(\vec{p}_i - \vec{p}_r)_T}{\vec{p}_{i_T}} = \frac{(\vec{v}_i - \vec{v}_r)_T}{\vec{v}_{i_T}}$$

where α_{NM} and α_{TM} are respectively normal and tangential differential momentum accommodation coefficients, subscript N refers to the normal component and subscript T to the tangential component. The velocity components are given (cf. Fig. 10) by

$$\vec{v}_{i_N} = \vec{v}_i \cos\theta_i$$

$$\vec{v}_{r_N} = \vec{v}_r \cos\phi \cos\theta_r$$

$$\vec{v}_{i_T} = \vec{v}_i \sin\theta_i$$

$$\vec{v}_{r_T} = -\vec{v}_r \cos\phi \sin\theta_r$$

Note that $\vec{v}_{i_N}$ and $\vec{v}_{r_N}$ are in opposite directions whereas $\vec{v}_{i_T}$ and $\vec{v}_{r_T}$ are in the same direction. The component $\vec{v}_{w_N}$ is evaluated by averaging the normal component $u\cos\theta$ for a half-Maxwellian velocity distribution. The fraction of particles leaving in solid angle $d\Omega$ ($= u^2 \sin\theta d\phi du$) is

$$\frac{4u \cos\theta}{\bar{u}} \left(\frac{m}{2\pi kT}\right)^{3/2} e^{-\frac{mu^2}{2kT}} u^2 \sin\theta d\theta d\phi du$$

TABLE - VII . THE DIFFERENTIAL ENERGY ACCOMMODATION COEFFICIENTS AND THE SPATIAL DENSITY DISTRIBUTION* FOR 7000 m/sec HELIUM BEAM SCATTERED FROM CLEANED 6061 - T6 ALUMINUM PLATE AT 0° INCIDENCE ANGLE.

ϕ \ θ_r	-75°	-60°	-45°	-30°	-15°	0°	15°	30°	45°	60°	75°
0°	43 1·65	43 3·3	56 6·6	55 7·73	55 7·78	55 7·82	55 7·78	55 7·73	56 6·6	43 3·3	43 1·65
15°	49 1·55	55 3·1	52 5·9	56 6·66	55 7·08	55 7·76	55 7·08	54 6·66	52 5·9	55 3·1	49 1·55
30°	56 1·2	63 2·4	54 4·4	56 5·55	55 6·71	55 7·62	55 6·71	56 5·55	54 4·4	63 2·4	56 1·2
45°	57 1·1	59 2·0	55 3·3	58 4·6	55 5·9	54 6·4	55 5·9	58 4·6	55 3·3	59 2·0	57 1·1
60°	56 0·6	54 1·2	49 2·0	43 2·4	45 3·1	46 3·3	45 3·1	43 2·4	49 2·0	54 1·2	56 0·6
75°	56 0·3	54 0·6	49 1·1	43 1·2	45 1·55	46 1·65	45 1·55	43 1·2	49 1·1	54 0·6	56 0·3

(a) DIFFERENTIAL ACCOMMODATION COEFFICIENT (%)

(b) SPATIAL DENSITY (ARBITRARY UNITS)

*MEASURED VALUES ARE UNDERLINED.

ORIGINAL PAGE IS
OF POOR QUALITY

TABLE - VIII. THE DIFFERENTIAL ENERGY ACCOMMODATION COEFFICIENTS AND THE SPATIAL DENSITY DISTRIBUTION* FOR 7000 m/sec HELIUM BEAM SCATTERED FROM CLEANED 6061 - T6 ALUMINUM PLATE AT 15° INCIDENCE ANGLE.

ϕ \ θ_r	-75°	-60°	-45°	-30°	-15°	0°	15°	30°	45°	60°	75°
0°	79 1·7	<u>79</u> <u>3·4</u>	54 7·92	50 7·4	46 6·97	47 7·10	47 7·46	<u>48</u> <u>7·1</u>	<u>46</u> <u>4·8</u>	<u>38</u> <u>3·0</u>	38 1·5
15°	70 1·65	<u>70</u> <u>3·3</u>	59 7·37	52 7·70	50 7·14	47 6·52	46 6·29	<u>48</u> <u>5·9</u>	<u>30</u> <u>4·3</u>	<u>35</u> <u>2·2</u>	36 1·1
30°	77 1·4	<u>77</u> <u>2·8</u>	65 5·63	54 7·33	52 7·37	48 6·47	45 5·52	<u>47</u> <u>5·0</u>	<u>45</u> <u>3·4</u>	40 2·01	38 1·14
45°	80 1·15	<u>80</u> <u>2·3</u>	<u>76</u> <u>3·4</u>	<u>57</u> <u>6.1</u>	<u>55</u> <u>6·8</u>	<u>52</u> <u>6·3</u>	<u>43</u> <u>4·8</u>	<u>42</u> <u>3·4</u>	43 2·55	42 1·51	40 0·85
60°	77 0·8	<u>77</u> <u>1·6</u>	<u>83</u> <u>2·3</u>	<u>61</u> <u>4·6</u>	<u>62</u> <u>4.8</u>	<u>60</u> <u>4·6</u>	<u>55</u> <u>3·9</u>	48 2·69	46 2.02	44 1·22	42 0·76
75°	77 0·4	77 0·80	83 1·15	61 2·3	62 2·4	60 2·3	55 1·95	48 1·14	46 0·85	44 0·44	42 0·30

(a) DIFFERENTIAL ACCOMMODATION COEFFICIENT (%)

(b) SPATIAL DENSITY (ARBITRARY UNITS)

*MEASURED VALUES ARE UNDERLINED.

ORIGINAL PAGE IS
OF POOR QUALITY

TABLE - IX . THE DIFFERENTIAL ENERGY ACCOMMODATION COEFFICIENTS AND THE SPATIAL DENSITY DISTRIBUTION* FOR 7000 m/sec HELIUM BEAM SCATTERED FROM CLEANED 6061 - T6 ALUMINUM PLATE AT 30° INCIDENCE ANGLE.

ϕ \ θ_r	-75°	-60°	-45°	-30°	-15°	0°	15°	30°	45°	60°	75°
0°	58 1·6	57 6·27	55 7·22	53 7·73	52 8·20	51 8·49	51 8·2	42 7·2	34 4·0	45 2·4	45 1·2
15°	41 1·6	60 4·82	57 6·21	55 6·99	53 7·30	51 7·62	48 7·6	38 6·2	40 3·8	50 2·2	47 1·1
30°	52 1·3	63 3·28	59 4·72	57 6·15	55 6·37	53 6·3	47 6·0	40 5·0	37 3·4	43 2·02	45 1·14
45°	59 1·0	67 2·2	60 3·0	59 4·8	57 5·2	60 5·0	49 4·0	40 3·4	38 2·55	41 1·51	43 0·85
60°	62 0·7	65 1·5	64 2·2	55 2·6	63 3·0	49 2·8	50 2·4	45 2·10	42 1·57	41 0·92	42 0·48
75°	62 0·4	65 0·8	64 1·1	55 1·3	63 1·5	49 1·4	50 1·2	45 1·14	42 0·55	41 0·44	42 0·22

(a) DIFFERENTIAL ACCOMMODATION COEFFICIENT (%)

(b) SPATIAL DENSITY (ARBITRARY UNITS)

*MEASURED VALUES ARE UNDERLINED.

ORIGINAL PAGE IS
OF POOR QUALITY

TABLE - X . THE DIFFERENTIAL ENERGY ACCOMMODATION COEFFICIENTS AND THE SPATIAL DENSITY DISTRIBUTION+ FOR 7000 m/sec HELIUM BEAM SCATTERED FROM CLEANED 6061 - T6 ALUMINUM PLATE AT 45° INCIDENCE ANGLE.

ϕ \ θ_r	-75°	-60°	-45°	-30°	-15°	0°	15°	30°	45°	60°	75°
0°	59 5·13	57 5·60	52 5·95	49 6·45	47 6·85	49 6·7	55 5·9	51 5·2	47 3·7	19 2·2	19 1·1
15°	62 4·15	62 5·06	56 5·39	50 5·62	45 6·04	42 6·3	41 5·8	37 4·9	34 3·5	25 1·9	22 0·95
30°	61 2·77	68 4·16	62 4·88	54 4·92	49 4·92	39 5·2	38 4·8	25 4·1	36 3·2	30 1·81	26 1·0
45°	55 1·5	74 2·8	69 3·9	60 4·1	59 3·7	37 3·7	34 3·5	23 3·2	29 2·4	30 1·37	28 0·8
60°	61 1·0	67 1·5	56 2·0	60 2·2	58 2·2	21 2·2	27 2·06	25 1·78	27 1·35	29 0·75	28 0·36
75°	61 0·5	67 0·75	56 1·0	60 1·1	58 1·1	21 1·1	27 1·1	25 1·0	27 0·8	29 0·38	28 0·19

(a) DIFFERENTIAL ACCOMMODATION COEFFICIENT (%)

(b) SPATIAL DENSITY (ARBITRARY UNITS)

+MEASURED VALUES ARE UNDERLINED

TABLE -XI . THE DIFFERENTIAL ENERGY ACCOMMODATION COEFFICIENTS AND THE SPATIAL DENSITY DISTRIBUTION* FOR 7000 m/sec HELIUM BEAM SCATTERED FROM CLEANED 60GI-T6 ALUMINUM PLATE AT 60° INCIDENCE ANGLE.

ϕ \ θ_r	-75°	-60°	-45°	-30°	-15°	0°	15°	30°	45°	60°	75°
0°	66 4·53	66 5·29	66 5·93	65 6·29	62 6·2	58 5·8	63 5·5	66 5·2	51 5.0	51 3·33	51 1·67
15°	66 3·67	66 4·41	66 5·10	68 5·69	68 6·0	71 5·6	75 5·2	53 5·0	52 4·5	51 3·0	51 1·5
30°	67 2·85	65 3·55	65 4·24	68 4·72	70 5.0	74 4.9	73 4·8	56 4·5	54 3·5	53 2·3	52 1·2
45°	69 2·0	65 2·6	61 3·4	67 3·8	66 4·0	74 4·0	73 3·45	65 3·0	59 2·3	56 1·2	54 0·6
60°	64 1·0	60 1·6	72 2·4	70 2·6	68 2·67	71 2·67	72 2·31	68 2·04	64 1·57	60 0·89	57 0·46
75°	64 0·5	60 0·8	72 1·2	70 1·3	68 1·33	71 1·33	72 1·15	66 1·04	64 0·78	60 0·45	57 0·23

(a) DIFFERENTIAL ACCOMMODATION COEFFICIENT (%)

(b) SPATIAL DENSITY (ARBITRARY UNITS)

*MEASURED VALUES ARE UNDERLINED.

ORIGINAL PAGE IS
OF POOR QUALITY

ORIGINAL PAGE IS
OF POOR QUALITY

TABLE - XII . THE DIFFERENTIAL ENERGY ACCOMMODATION COEFFICIENTS AND THE SPATIAL DENSITY DISTRIBUTION* FOR 7000 m/sec HELIUM BEAM SCATTERED FROM CLEANED 6061 - T6 ALUMINUM PLATE AT 75° INCIDENCE ANGLE.

ϕ \ θ_r	-75°	-60°	-45°	-30°	-15°	0°	15°	30°	45°	60°	75°
0°	76 5.07	74 6.27	72 6.93	72 7.0	66 6.1	64 5.4	51 5.0	50 4.8	45 4.5	45 3.0	45 1.5
15°	78 3.65	76 4.92	72 5.87	63 6.1	70 5.8	63 5.2	59 4.9	59 4.5	52 3.57	48 2.3	47 1.2
30°	80 2.54	80 3.45	82 4.8	80 5.4	60 5.0	53 4.5	56 3.82	57 3.30	55 2.62	52 1.50	49 0.75
45°	79 1.9	79 2.2	84 3.4	78 3.9	58 4.0	55 3.4	56 2.85	57 2.45	56 1.92	54 1.0	51 0.5
60°	66 1.1	78 1.8	73 2.2	75 2.5	52 2.5	54 2.22	55 1.84	56 1.61	56 1.28	55 0.75	53 0.35
75°	66 0.55	78 0.9	73 1.1	75 1.25	52 1.25	54 1.2	55 0.90	56 0.90	56 0.75	55 0.50	53 0.25

(a) DIFFERENTIAL ACCOMMODATION COEFFICIENT (%)

(b) SPATIAL DENSITY (ARBITRARY UNITS)

*MEASURED VALUES ARE UNDERLINED.

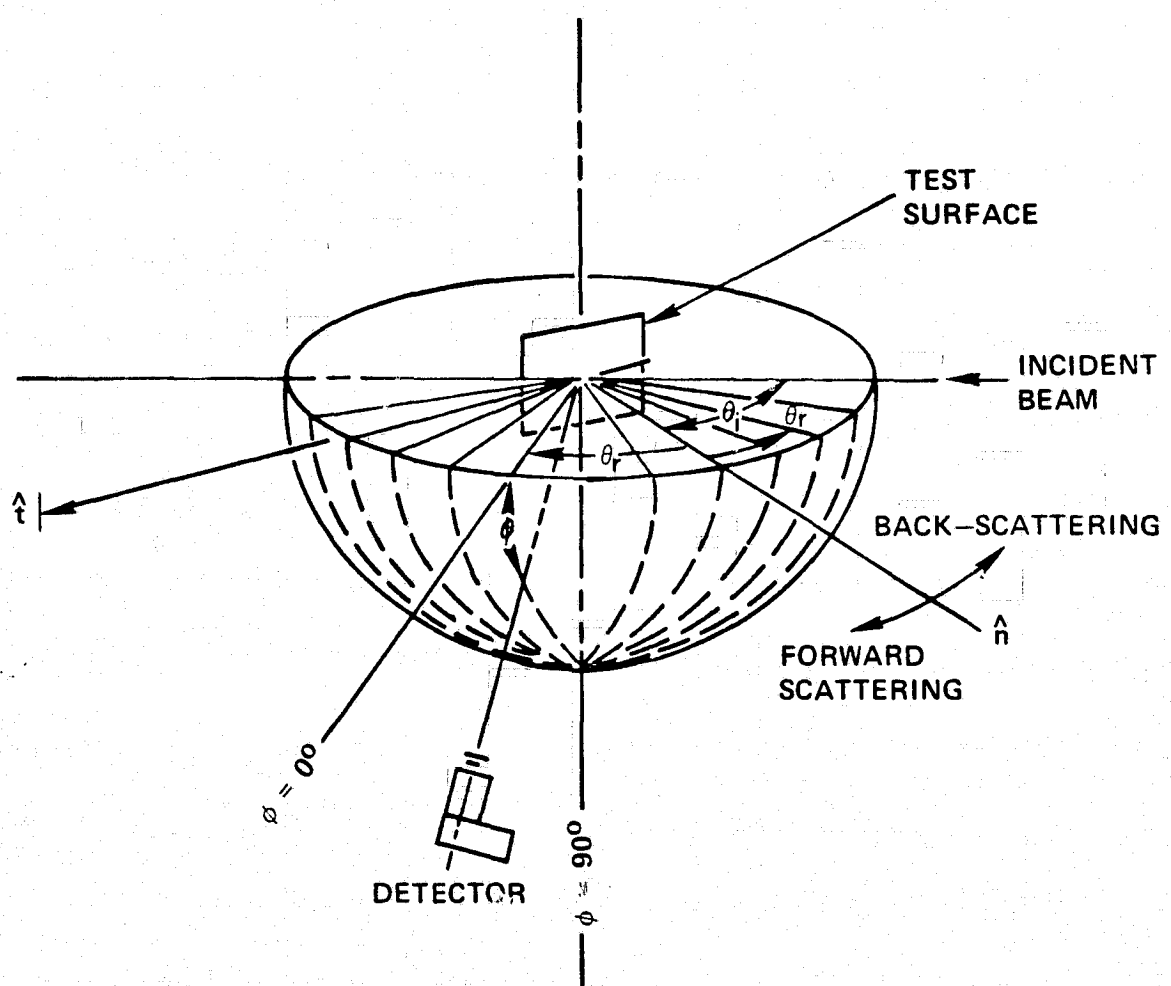

Figure 10. Schematic Diagram of the Scattering System.

Hence

$$\vec{v}_{W_N} = \int_0^{\infty} \int_0^{\pi/2} \int_0^{2\pi} u \cos\theta \, \frac{4u\cos\theta}{\bar{u}} \left(\frac{m}{2\pi kT}\right)^{3/2} e^{-\frac{mu^2}{2kT}} u^2 \sin\theta \, d\theta \, d\phi \, du$$

$$= \sqrt{\frac{\pi}{2} \frac{kT}{m}}$$

The direction of $\vec{v}_{W_N}$ also is opposite to that of $\vec{v}_{i_N}$.

The computed values of the differential normal and tangential momentum accommodation coefficients are given in Tables XIII - XVIII.

Overall Normal and Tangential Momentum Accommodation Coefficients

Overall normal and tangential momentum-accommodation coefficients $\bar{\alpha}$ were calculated for each incidence angle by averaging over the differential coefficients α_i taking into account the flux distribution and the solid angle represented by each measurement. Thus, the overall accommodation coefficient was deduced from the differential coefficients using

$$\bar{\alpha} = \frac{\sum_i j_i \alpha_i (\Delta w)_i}{\sum_i j_i (\Delta w)_i}$$

where j_i is the flux and $(\Delta w)_i$ is the solid angle corresponding to the measurement. Since j_i is proportional to $n_i\sqrt{1-\alpha_{E_i}}$ and $(\Delta w)_i$ to $\cos\phi_i$, one may write

$$\bar{\alpha} = \frac{\sum_i n_i\sqrt{1-\alpha_{E_i}} \, \alpha_i \cos\phi_i}{\sum_i n_i\sqrt{1-\alpha_{E_i}} \cos\phi_i}$$

where n_i is the number density, α_{E_i} is the energy-accommodation coefficient, and ϕ_i is the out-of-plane scattering angle measured from the plane of incidence.

The deduced values are plotted as a function of incidence angle θ_i in Fig. 11.

TABLES XIII - XVIII

DIFFERENTIAL NORMAL AND TANGENTIAL MOMENTUM ACCOMMODATION COEFFICIENTS

In the following tables:

α_E = differential energy accommodation coefficient

n = spatial density

α_{NM} = differential normal momentum accommodation coefficient

α_{TM} = differential tangential momentum accommodation coefficient

ORIGINAL PAGE IS
OF POOR QUALITY

TABLE - XIII. $\theta_i = 0°$

ϕ RUN PHI	θ_R TH(R)	α_E EAC	π ND	α_{NM} ACNM
0.0	-60.0	0.41	0.0330	1.21
0.0	-45.0	0.56	0.0660	1.29
0.0	45.0	0.56	0.0660	1.29
0.0	60.0	0.43	0.0330	1.21
0.0	-75.0	0.43	0.0160	1.05
0.0	-30.0	0.55	0.0770	1.39
0.0	-15.0	0.55	0.0770	1.45
0.0	0.0	0.55	0.0780	1.47
0.0	15.0	0.55	0.0770	1.45
0.0	30.0	0.55	0.0770	1.39
0.0	75.0	0.43	0.0160	1.05
15.0	-60.0	0.55	0.0310	1.16
15.0	-45.0	0.52	0.0590	1.29
15.0	45.0	0.52	0.0590	1.29
15.0	60.0	0.55	0.0310	1.16
30.0	-60.0	0.53	0.0240	1.11
30.0	-45.0	0.54	0.0440	1.24
30.0	45.0	0.54	0.0440	1.24
30.0	60.0	0.53	0.0240	1.11
45.0	-45.0	0.55	0.0330	1.17
45.0	-30.0	0.58	0.0460	1.23
45.0	-15.0	0.55	0.0590	1.28
45.0	0.0	0.54	0.0540	1.30
45.0	15.0	0.55	0.0590	1.28
45.0	30.0	0.58	0.0460	1.23
45.0	45.0	0.55	0.0330	1.17
60.0	-30.0	0.43	0.0240	1.17
60.0	-15.0	0.45	0.0310	1.19
60.0	0.0	0.46	0.0330	1.20
60.0	15.0	0.45	0.0310	1.19
60.0	30.0	0.43	0.0240	1.17
15.0	-75.0	0.49	0.0150	1.04
15.0	-30.0	0.56	0.0660	1.37
15.0	-15.0	0.55	0.0700	1.43
15.0	0.0	0.55	0.0770	1.45
15.0	15.0	0.55	0.0700	1.43
15.0	30.0	0.54	0.0660	1.38
15.0	75.0	0.49	0.0150	1.04
30.0	-75.0	0.56	0.0120	1.01
30.0	-30.0	0.55	0.0550	1.32
30.0	-15.0	0.55	0.0670	1.37
30.0	0.0	0.55	0.0760	1.39
30.0	15.0	0.55	0.0670	1.37
30.0	30.0	0.56	0.0550	1.32
30.0	75.0	0.56	0.0120	1.01
45.0	-75.0	0.57	0.0110	0.98
45.0	-60.0	0.59	0.0200	1.08
45.0	60.0	0.59	0.0200	1.08
45.0	75.0	0.57	0.0110	0.98
60.0	-75.0	0.56	0.0060	0.95
60.0	-60.0	0.54	0.0120	1.03
60.0	-45.0	0.49	0.0200	1.10
60.0	45.0	0.49	0.0200	1.10
60.0	60.0	0.54	0.0120	1.03
60.0	75.0	0.56	0.0060	0.95
75.0	-75.0	0.56	0.0030	0.92
75.0	-60.0	0.54	0.0060	0.96
75.0	-45.0	0.49	0.0110	0.99
75.0	-30.0	0.43	0.0120	1.03
75.0	-15.0	0.45	0.0150	1.04
75.0	0.0	0.46	0.0160	1.05
75.0	15.0	0.45	0.0150	1.04
75.0	30.0	0.43	0.0120	1.03
75.0	45.0	0.49	0.0110	0.99
75.0	60.0	0.54	0.0060	0.96
75.0	75.0	0.56	0.0030	0.92

TABLE - XIV. $\theta_i = 15°$

ϕ PHI	θ_R TH(R)	α_E AC	n ND	α_{NM} ACNM	α_{TM} ACTM
0.0	-60.0	0.79	0.034	1.08	2.53
0.0	30.0	0.48	0.071	1.44	-0.39
0.0	45.0	0.46	0.048	1.35	-1.01
0.0	60.0	0.38	0.030	1.23	-1.63
0.0	-75.0	0.79	0.017	0.98	-2.71
0.0	-45.0	0.54	0.079	1.31	2.85
0.0	-30.0	0.50	0.074	1.43	2.37
0.0	-15.0	0.48	0.069	1.51	1.72
0.0	0.0	0.47	0.071	1.53	1.00
0.0	15.0	0.47	0.074	1.51	0.27
0.0	75.0	0.38	0.015	1.06	-1.94
15.0	-60.0	0.70	0.033	1.11	2.77
15.0	30.0	0.48	0.059	1.42	-0.35
15.0	45.0	0.30	0.043	1.39	-1.21
15.0	60.0	0.35	0.022	1.23	-1.61
30.0	-60.0	0.77	0.028	1.06	2.39
30.0	30.0	0.47	0.050	1.37	-0.22
30.0	45.0	0.45	0.034	1.29	-0.75
45.0	-60.0	0.49	0.023	1.02	2.06
45.0	-45.0	0.75	0.034	1.10	1.95
45.0	-30.0	0.57	0.061	1.24	1.90
45.0	-15.0	0.55	0.068	1.29	1.47
45.0	0.0	0.52	0.063	1.32	1.01
45.0	15.0	0.43	0.048	1.34	0.47
45.0	30.0	0.42	0.034	1.33	-0.04
60.0	-60.0	0.77	0.016	0.98	1.80
60.0	-45.0	0.43	0.023	1.01	1.55
60.0	-30.0	0.41	0.046	1.12	1.80
60.0	-15.0	0.52	0.048	1.15	1.31
60.0	0.0	0.50	0.045	1.16	1.00
60.0	15.0	0.55	0.039	1.17	0.66
15.0	-75.0	0.70	0.016	1.00	2.47
15.0	-45.0	0.59	0.073	1.27	2.69
15.0	-30.0	0.52	0.077	1.40	2.29
15.0	-15.0	0.50	0.071	1.47	1.68
15.0	0.0	0.47	0.065	1.51	1.00
15.0	15.0	0.46	0.062	1.50	0.29
15.0	75.0	0.35	0.011	1.06	-1.83
30.0	-75.0	0.77	0.014	0.97	2.55
30.0	-45.0	0.55	0.059	1.20	2.40
30.0	-30.0	0.54	0.073	1.34	2.13
30.0	-15.0	0.52	0.073	1.40	1.60
30.0	0.0	0.48	0.064	1.44	1.00
30.0	15.0	0.45	0.055	1.44	0.36
30.0	60.0	0.40	0.020	1.18	-1.24
30.0	75.0	0.38	0.011	1.04	-1.55
45.0	-75.0	0.80	0.011	0.95	2.18
45.0	45.0	0.43	0.020	1.22	-0.46
45.0	60.0	0.42	0.015	1.12	-0.80
45.0	75.0	0.40	0.008	1.00	-1.04
60.0	-75.0	0.77	0.008	0.93	1.90
60.0	30.0	0.48	0.026	1.16	0.30
60.0	45.0	0.45	0.020	1.11	-0.02
60.0	60.0	0.44	0.012	1.04	-0.25
60.0	75.0	0.42	0.007	0.96	-0.42
75.0	-75.0	0.77	0.004	0.90	1.46
75.0	-60.0	0.77	0.008	0.93	1.42
75.0	-45.0	0.33	0.011	0.94	1.29
75.0	-30.0	0.51	0.023	1.00	1.31
75.0	-15.0	0.52	0.024	1.01	1.16
75.0	0.0	0.50	0.023	1.02	1.00
75.0	15.0	0.55	0.019	1.03	0.83
75.0	30.0	0.48	0.011	1.02	0.64
75.0	45.0	0.45	0.008	1.00	0.48
75.0	60.0	0.44	0.004	0.96	0.35
75.0	75.0	0.42	0.003	0.92	0.26

ORIGINAL PAGE IS
OF POOR QUALITY

TABLE - XV. $\theta_i = 30^\circ$

ϕ	θ_R	α_E	n	α_{NM}	α_{TM}
RUN					
PAI	TH(R)	EAC	ND	ACNM	ACTM
0.0	-75.0	0.59	0.01550	1.03	2.25
0.0	15.0	0.51	0.03820	1.54	0.64
0.0	30.0	0.42	0.07220	1.52	0.24
0.0	45.0	0.34	0.04000	1.44	-0.15
0.0	60.0	0.45	0.03940	1.23	-0.28
0.0	-60.0	0.57	0.06220	1.19	2.14
0.0	-45.0	0.55	0.07220	1.34	1.95
0.0	-30.0	0.53	0.07770	1.45	1.69
0.0	-15.0	0.52	0.03820	1.54	1.36
0.0	0.0	0.51	0.03840	1.56	1.00
0.0	75.0	0.45	0.00120	1.05	-0.43
15.0	-75.0	0.41	0.00150	1.00	2.43
15.0	15.0	0.48	0.00750	1.53	0.64
15.0	30.0	0.38	0.00520	1.52	0.24
15.0	45.0	0.40	0.00380	1.39	-0.06
15.0	60.0	0.50	0.00220	1.20	-0.18
30.0	15.0	0.47	0.00300	1.47	0.07

30.0	30	0.40	0.0300	1.44	0.33
30.0	45.0	0.37	0.0340	1.35	0.03
45.0	-60.0	0.37	0.0220	1.07	1.70
45.0	-45.0	0.39	0.0360	1.16	1.63
45.0	-30.0	0.39	0.0480	1.25	1.45
45.0	-15.0	0.37	0.0520	1.31	1.24
45.0	0.0	0.50	0.0500	1.31	1.00
45.0	15.0	0.49	0.0400	1.30	0.74
45.0	30.0	0.40	0.0340	1.34	0.45
60.0	-45.0	0.34	0.0220	1.07	1.42
60.0	-30.0	0.35	0.0260	1.15	1.34
60.0	-15.0	0.33	0.0300	1.16	1.16
60.0	0.0	0.49	0.0280	1.22	1.00
60.0	15.0	0.50	0.0240	1.20	0.82
60.0	30.0	0.50	0.0480	1.17	2.06
15.0	-60.0	0.57	0.0520	1.31	1.90
15.0	-45.0	0.55	0.0500	1.42	1.65
15.0	-30.0	0.53	0.0730	1.50	1.34
15.0	-15.0	0.51	0.0760	1.54	1.00
15.0	0.0	0.47	0.0110	1.04	-0.30
15.0	75.0	0.52	0.0130	1.02	2.15
30.0	-75.0	0.53	0.0320	1.13	1.91
30.0	-60.0	0.59	0.0470	1.25	1.78
30.0	-45.0	0.57	0.0510	1.35	1.57
30.0	-30.0	0.55	0.0530	1.42	1.30
30.0	-15.0	0.53	0.0530	1.45	1.00
30.0	0.0	0.43	0.0200	1.19	-0.13
30.0	60.0	0.45	0.0110	1.03	-0.24
30.0	75.0	0.59	0.0100	0.98	1.87
45.0	-75.0	0.38	0.0250	1.23	0.21
45.0	45.0	0.41	0.0155	1.13	0.05
45.0	60.0	0.43	0.0080	1.00	-0.03
45.0	75.0	0.52	0.0070	0.94	1.60
60.0	-75.0	0.55	0.0150	1.01	1.51
60.0	-60.0	0.45	0.0200	1.18	0.53
60.0	30.0	0.42	0.0150	1.13	0.46
60.0	45.0	0.41	0.0090	1.05	0.33
60.0	60.0	0.42	0.0040	0.98	0.26
60.0	75.0	0.52	0.0040	0.90	1.91
75.0	-75.0	0.55	0.0080	0.94	1.27
75.0	-60.0	0.54	0.0110	0.97	1.22
75.0	-45.0	0.55	0.0130	1.01	1.17
75.0	-30.0	0.53	0.0150	1.01	1.08
75.0	-15.0	0.43	0.0140	1.06	1.00
75.0	0.0	0.50	0.0120	1.04	0.91
75.0	15.0	0.45	0.0110	1.03	0.81
75.0	30.0	0.42	0.0080	1.00	0.72
75.0	45.0	0.41	0.0040	0.96	0.58
75.0	60.0	0.42	0.0020	0.91	0.62
75.0	75.0				

ORIGINAL PAGE IS
OF POOR QUALITY

TABLE - XVI . $\theta i = 45°$

ϕ + RUN PHI	θ_R TH(R)	α_E EAC	n ND	α_{NM} ACNM	α_{TM} ACTM
0.0	0.0	0.49	0.0570	1.68	1.00
0.0	15.0	0.55	0.0590	1.60	0.75
0.0	30.0	0.51	0.0520	1.55	0.51
0.0	45.0	0.47	0.0370	1.45	0.27
0.0	60.0	0.19	0.0220	1.37	-0.10
0.0	-75.0	0.59	0.0510	1.03	1.87
0.0	-60.0	0.57	0.0560	1.23	1.80
0.0	-45.0	0.52	0.0590	1.42	1.59
0.0	-30.0	0.49	0.0640	1.57	1.50
0.0	-15.0	0.47	0.0680	1.67	1.27
0.0	75.0	0.19	0.0110	1.11	-0.23
15.0	0.0	0.42	0.0630	1.71	1.00
15.0	15.0	0.41	0.0580	1.69	0.73
15.0	30.0	0.37	0.0490	1.62	0.46
15.0	45.0	0.34	0.0350	1.49	0.22
15.0	60.0	0.25	0.0190	1.33	-0.02
30.0	0.0	0.39	0.0520	1.64	1.00
30.0	15.0	0.38	0.0480	1.62	0.75
30.0	30.0	0.25	0.0410	1.61	0.47
30.0	45.0	0.36	0.0320	1.42	0.31
45.0	-75.0	0.55	0.0150	0.98	1.65
45.0	-60.0	0.74	0.0280	1.05	1.44
45.0	-45.0	0.59	0.0390	1.17	1.39
45.0	-30.0	0.60	0.0410	1.30	1.32
45.0	-15.0	0.59	0.0370	1.35	1.17
45.0	0.0	0.37	0.0370	1.50	1.00
45.0	15.0	0.34	0.0350	1.49	0.79
45.0	30.0	0.23	0.0320	1.47	0.56
60.0	-60.0	0.67	0.0150	1.01	1.35
60.0	-45.0	0.56	0.0200	1.11	1.33
60.0	-30.0	0.60	0.0220	1.16	1.22
60.0	-15.0	0.58	0.0220	1.21	1.12
60.0	0.0	0.21	0.0220	1.36	1.00
15.0	-75.0	0.62	0.0410	1.02	1.81
15.0	-60.0	0.62	0.0500	1.19	1.73
15.0	-45.0	0.56	0.0530	1.37	1.64
15.0	-30.0	0.50	0.0560	1.54	1.48
15.0	-15.0	0.45	0.0600	1.66	1.26
15.0	75.0	0.22	0.0090	1.10	-0.17
30.0	-75.0	0.61	0.0270	1.00	1.74
30.0	-60.0	0.68	0.0410	1.13	1.60
30.0	-45.0	0.62	0.0480	1.28	1.53
30.0	-30.0	0.54	0.0490	1.44	1.42
30.0	-15.0	0.49	0.0490	1.54	1.23
30.0	60.0	0.30	0.0180	1.27	0.11
30.0	75.0	0.26	0.0100	1.07	-0.02
45.0	45.0	0.29	0.0240	1.34	0.40
45.0	60.0	0.30	0.0130	1.19	0.28
45.0	75.0	0.23	0.0080	1.02	0.18
60.0	-75.0	0.61	0.0100	0.93	1.43
60.0	15.0	0.27	0.0200	1.33	0.84
60.0	30.0	0.25	0.0170	1.28	0.69
60.0	45.0	0.27	0.0130	1.19	0.57
60.0	60.0	0.29	0.0070	1.09	0.48
60.0	75.0	0.28	0.0030	0.97	0.42
75.0	-75.0	0.61	0.0050	0.89	1.22
75.0	-60.0	0.67	0.0070	0.93	1.18
75.0	-45.0	0.56	0.0100	0.98	1.17
75.0	-30.0	0.60	0.0110	1.00	1.12
75.0	-15.0	0.58	0.0110	1.03	1.06
75.0	0.0	0.21	0.0110	1.11	1.00
75.0	15.0	0.27	0.0110	1.09	0.92
75.0	30.0	0.25	0.0100	1.07	0.84
75.0	45.0	0.27	0.0080	1.02	0.78
75.0	60.0	0.29	0.0030	0.97	0.73
75.0	75.0	0.28	0.0010	0.90	0.70

ORIGINAL PAGE IS
OF POOR QUALITY

TABLE - XVII. $\theta_i = 60^\circ$

ϕ , RUN	θ_R	α_E	n	α_{NM}	α_{TM}
PHI	TH(R)	EAC	ND	ACNM	ACTM
0.0	-15.0	0.62	0.0620	1.72	1.18
0.0	0.0	0.58	0.0580	1.80	1.00
0.0	15.0	0.63	0.0550	1.71	0.82
0.0	30.0	0.66	0.0520	1.58	0.66
0.0	45.0	0.51	0.0500	1.56	0.43
0.0	-75.0	0.66	0.0450	1.02	1.65
0.0	-60.0	0.65	0.0520	1.24	1.58
0.0	-45.0	0.66	0.0590	1.43	1.48
0.0	-30.0	0.65	0.0620	1.59	1.34
0.0	60.0	0.51	0.0330	1.33	0.30
0.0	75.0	0.51	0.0160	1.07	0.22
15.0	-15.0	0.68	0.0600	1.61	1.16
15.0	0.0	0.71	0.0560	1.60	1.00
15.0	15.0	0.75	0.0520	1.52	0.86
15.0	30.0	0.53	0.0500	1.68	0.62
15.0	45.0	0.52	0.0450	1.53	0.45
30.0	-15.0	0.70	0.0600	1.50	1.14
30.0	0.0	0.74	0.0490	1.48	1.00
30.0	15.0	0.73	0.0480	1.47	0.87
30.0	30.0	0.55	0.0450	1.56	0.67
45.0	-75.0	0.59	0.0200	0.94	1.44
45.0	-60.0	0.65	0.0260	1.11	1.42
45.0	-45.0	0.61	0.0340	1.27	1.36
45.0	-30.0	0.67	0.0380	1.34	1.23
45.0	-15.0	0.56	0.0400	1.41	1.12
45.0	0.0	0.74	0.0400	1.35	1.00
60.0	-60.0	0.60	0.0160	1.03	1.32
60.0	-45.0	0.72	0.0240	1.08	1.22
60.0	-30.0	0.70	0.0260	1.16	1.16
15.0	-75.0	0.66	0.0360	1.01	1.63
15.0	-60.0	0.65	0.0440	1.23	1.56
15.0	-45.0	0.66	0.0510	1.41	1.46
15.0	-30.0	0.68	0.0550	1.53	1.32
15.0	60.0	0.51	0.0300	1.31	0.32
15.0	75.0	0.51	0.0150	1.06	0.25
30.0	-75.0	0.67	0.0280	0.99	1.55
30.0	-60.0	0.65	0.0350	1.19	1.51
30.0	-45.0	0.65	0.0420	1.35	1.42
30.0	-30.0	0.63	0.0470	1.45	1.28
30.0	45.0	0.54	0.0350	1.44	0.52
30.0	60.0	0.53	0.0230	1.25	0.41
30.0	75.0	0.52	0.0120	1.03	0.33
45.0	15.0	0.73	0.0340	1.34	0.89
45.0	30.0	0.65	0.0300	1.35	0.76
45.0	45.0	0.59	0.0230	1.29	0.63
45.0	60.0	0.56	0.0120	1.15	0.53
45.0	75.0	0.54	0.0060	0.98	0.47
60.0	-75.0	0.64	0.0100	0.91	1.33
60.0	-15.0	0.68	0.0260	1.21	1.08
60.0	0.0	0.71	0.0260	1.21	1.00
60.0	15.0	0.72	0.0230	1.18	0.92
60.0	30.0	0.53	0.0200	1.17	0.84
60.0	45.0	0.64	0.0150	1.12	0.76
60.0	60.0	0.60	0.0080	1.03	0.68
60.0	75.0	0.57	0.0040	0.92	0.63
75.0	-75.0	0.64	0.0050	0.85	1.17
75.0	-60.0	0.60	0.0080	0.91	1.16
75.0	-45.0	0.72	0.0120	0.94	1.11
75.0	-30.0	0.70	0.0130	0.98	1.08
75.0	-15.0	0.68	0.0130	1.01	1.04
75.0	0.0	0.71	0.0130	1.00	1.00
75.0	15.0	0.72	0.0110	0.99	0.96
75.0	30.0	0.53	0.0100	0.98	0.92
75.0	45.0	0.64	0.0070	0.96	0.87
75.0	60.0	0.60	0.0040	0.91	0.84
75.0	75.0	0.57	0.0020	0.85	0.81

ORIGINAL PAGE IS
OF POOR QUALITY

TABLE - XVIII $\theta_i = 75°$

ϕ *R'JN	θ_R	α_E	n	α_{NM}	α_{TM}
PHI	TH(R)	EAC	ND	ACNM	ACTM
0.0	-30.0	0.72	0.0700	1.81	1.27
0.0	-15.0	0.66	0.0610	2.07	1.16
0.0	0.0	0.64	0.0540	2.17	1.00
0.0	15.0	0.51	0.0500	2.36	0.81
0.0	30.0	0.50	0.0480	2.20	0.63
0.0	45.0	0.45	0.0450	1.98	0.46
0.0	-75.0	0.76	0.0500	0.97	1.49
0.0	-60.0	0.74	0.0620	1.30	1.46
0.0	-45.0	0.72	0.0690	1.60	1.39
0.0	60.0	0.45	0.0300	1.59	0.34
0.0	75.0	0.45	0.0150	1.14	0.26
15.0	-30.0	0.63	0.0510	1.94	1.30
15.0	-15.0	0.70	0.0580	1.94	1.14
15.0	0.0	0.63	0.0520	2.13	1.00
15.0	15.0	0.59	0.0490	2.16	0.83
15.0	30.0	0.59	0.0450	2.00	0.68
30.0	-30.0	0.30	0.0340	1.50	1.20
30.0	-15.0	0.60	0.0500	1.99	1.15
30.0	0.0	0.53	0.0450	2.15	1.00
45.0	-75.0	0.79	0.0190	0.86	1.32
45.0	-60.0	0.79	0.0220	1.06	1.29
45.0	-45.0	0.84	0.0340	1.16	1.21
45.0	-30.0	0.78	0.0390	1.38	1.17
45.0	-15.0	0.58	0.0400	1.77	1.12
60.0	-75.0	0.66	0.0110	0.84	1.29
60.0	-60.0	0.78	0.0180	0.95	1.21
60.0	-45.0	0.73	0.0220	1.12	1.19
60.0	-30.0	0.75	0.0250	1.20	1.13
60.0	-15.0	0.52	0.0250	1.50	1.09
15.0	-75.0	0.78	0.0360	0.95	1.45
15.0	-60.0	0.75	0.0490	1.25	1.42
15.0	-45.0	0.72	0.0580	1.56	1.37
15.0	45.0	0.52	0.0350	1.85	0.51
15.0	60.0	0.48	0.0230	1.53	0.38
15.0	75.0	0.46	0.0120	1.12	0.29
30.0	-75.0	0.80	0.0250	0.91	1.39
30.0	-60.0	0.80	0.0340	1.14	1.35
30.0	-45.0	0.82	0.0480	1.31	1.27
30.0	15.0	0.56	0.0380	2.05	0.85
30.0	30.0	0.57	0.0330	1.89	0.71
30.0	45.0	0.55	0.0260	1.69	0.57
30.0	60.0	0.52	0.0150	1.41	0.46
30.0	75.0	0.49	0.0070	1.06	0.38
45.0	0.0	0.55	0.0340	1.85	1.00
45.0	15.0	0.55	0.0290	1.80	0.87
45.0	30.0	0.57	0.0240	1.67	0.76
45.0	45.0	0.56	0.0190	1.49	0.66
45.0	60.0	0.54	0.0100	1.26	0.57
45.0	75.0	0.51	0.0050	0.98	0.50
60.0	0.0	0.54	0.0220	1.51	1.00
60.0	15.0	0.55	0.0180	1.47	0.91
60.0	30.0	0.56	0.0160	1.38	0.83
60.0	45.0	0.56	0.0120	1.24	0.76
60.0	60.0	0.55	0.0070	1.08	0.70
60.0	75.0	0.53	0.0030	0.88	0.66
75.0	-75.0	0.66	0.0050	0.75	1.15
75.0	-60.0	0.78	0.0090	0.81	1.11
75.0	-45.0	0.73	0.0110	0.89	1.10
75.0	-30.0	0.75	0.0120	0.94	1.07
75.0	-15.0	0.52	0.0120	1.09	1.05
75.0	0.0	0.54	0.0120	1.10	1.00
75.0	15.0	0.55	0.0090	1.08	0.95
75.0	30.0	0.56	0.0090	1.03	0.91
75.0	45.0	0.56	0.0070	0.96	0.87
75.0	60.0	0.56	0.0050	0.87	0.84
75.0	75.0	0.53	0.0020	0.77	0.82

ORIGINAL PAGE IS
OF POOR QUALITY

CLEANED 6061 T-6 Al

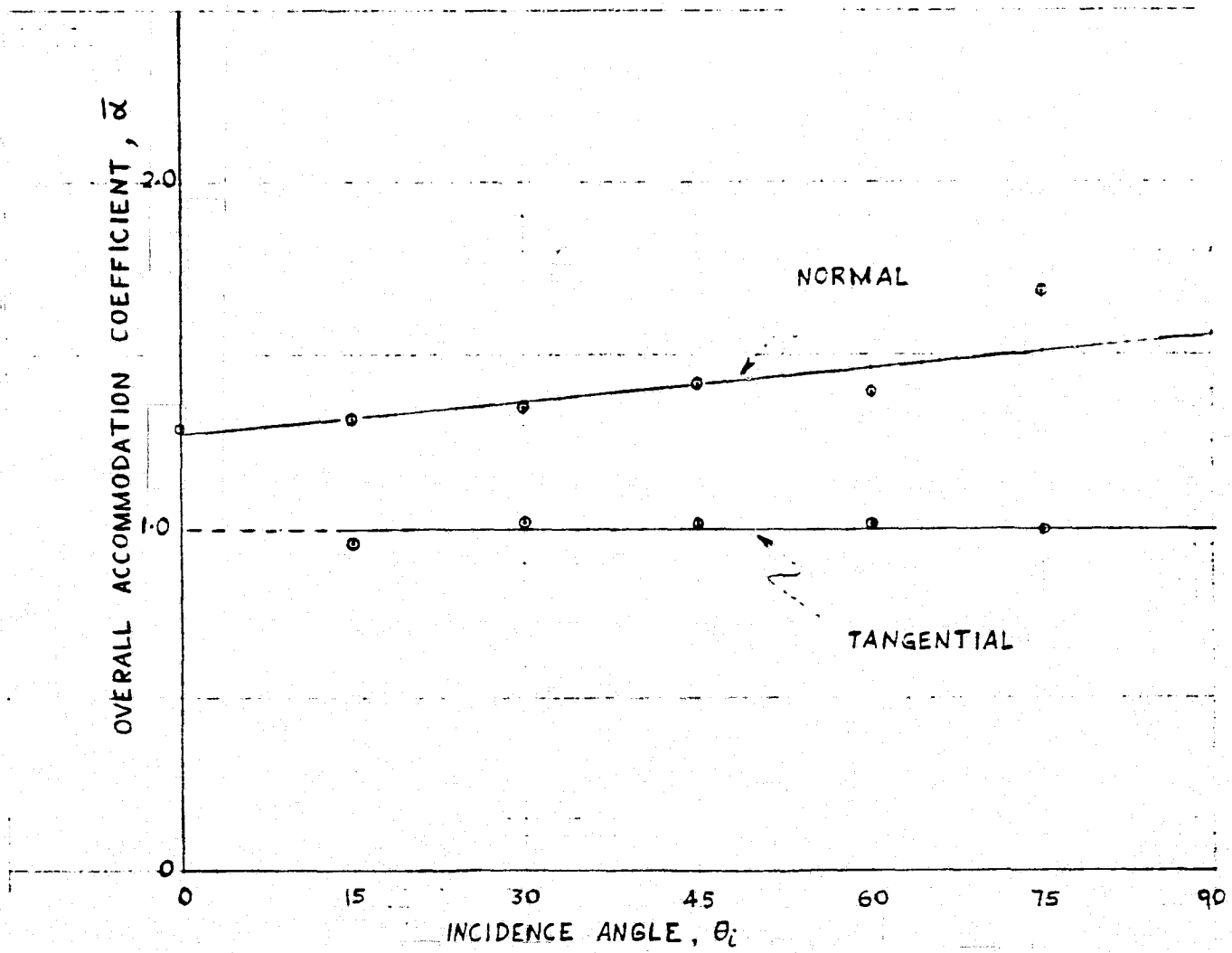

FIG. 11 OVERALL NORMAL AND TANGENTIAL MOMENTUM ACCOMMODATION COEFFICIENT AS A FUNCTION OF INCIDENCE ANGLE

Evaluation of Drag Coefficient for Spheres

An expression for the drag coefficient for spheres moving in a rarefied atmosphere was derived in terms of normal tangential momentum-accommodation coefficients. (See Appendix A.) For the case in which the molecular random thermal speeds in the atmosphere are negligible in comparison with the satellite speed, one obtains

$$C_D = \frac{4}{V_\infty} \sum_{\theta_i=0}^{\pi/2} \left[(V_\infty - V_w)_N \, (\alpha_{NM} \cos\theta_i) + (V_\infty - V_w)_T (\alpha_{TM} \sin\theta_i) \right] \times \sin\theta_i \cos\theta_i \, \Delta\theta_i$$

where α_{NM} and α_{TM} are, respectively, overall normal and tangential momentum-accommodation coefficients (a function of θ_i), V_∞ is the incident speed of the beam for which the experimental measurements are made, and V_w is the average reflected speed for complete accommodation with the surface.

The drag coefficient for 6061-T6 aluminum spheres was computed from the above expression using the results in Fig. 11 by numerical integration. (A computer program for this calculation is given in Appendix B.) For the given conditions (He impinging at 7000 m/sec), $C_D = 2.64$ was obtained.

The derivation of an expression that takes into account the molecular random thermal speeds in the atmosphere is more difficult. However, for the particular case when the normal and tangential momentum-accommodation coefficients are constant, a relatively simple expression for the drag coefficient may be derived in terms of the speed ratio, S. See, e.g., p. 167, Equation (16) of Patterson [4]. This predicted dependence on S, and some experimental points obtained for He, are shown in Fig. 12 (from Ref. 4). The good agreement between the predicted and the measured values establishes the trend of the variation of the drag coefficient with the speed ratio. Note also that in Fig. 12, for S greater than about 2.4,

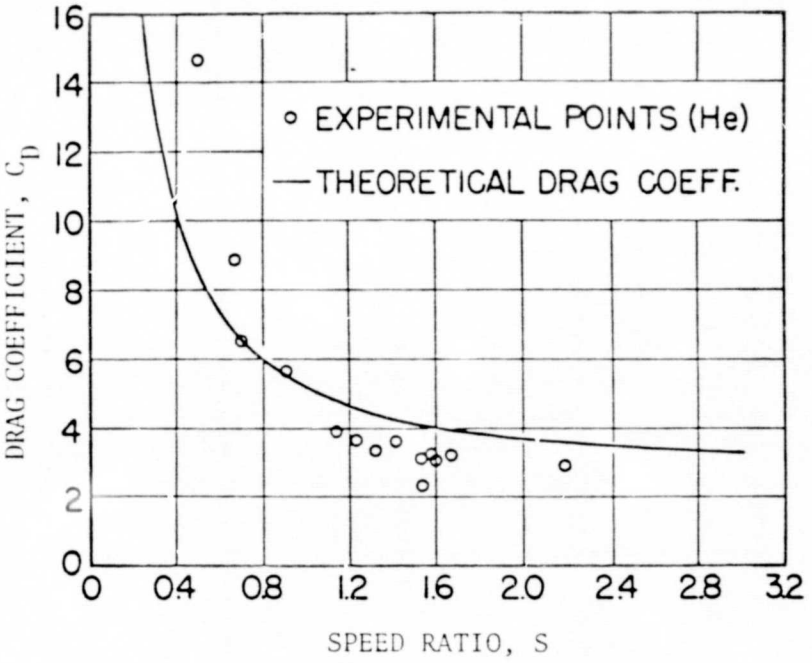

FIG. 12. Drag Coefficient as Function of Speed Ratio (from Fig. 38 of Ref. 4).

the drag coefficient approaches a terminal value and becomes relatively independent of the speed ratio.

For an atmospheric temperature of 1000°K, the speed ratio for a 7000 m/sec incident helium beam is 3.44. Thus, the expression for the drag coefficient given here is sufficiently accurate for many satellite conditions.

REFERENCES

1. Liu, S. M., W. E. Rodgers, and E. L. Knuth, "Interactions of Satellite-Speed Helium Atoms with Satellite Surfaces. I: Spatial Distributions of Reflected Surfaces," Report UCLA-ENG-7546. Los Angeles: UCLA School of Engineering and Applied Science, June 1975.

2. Liu, S. M., and E. L. Knuth, "Interactions of Satellite-Speed Helium Atoms with Satellite Surfaces. II: Energy Distribution of Reflected Helium Atoms," Report UCLA-ENG-7638. Los Angeles: UCLA School of Engineering and Applied Science, April 1976.

3. Young, W. S., "An Arc-Heated Ar-He Binary Supersonic Molecular Beam with Energies up to 21 ev," Report No. 69-39. Los Angeles: UCLA School of Engineering and Applied Science, July 1969.

4. Patterson, G. N., Introduction to the Kinetic Theory of Gas Flows. Toronto: University of Toronto Press, 1971.

APPENDIX A

Derivation of Drag Coefficient for Spheres for the Case of Infinite Speed Ratio

Consider a sphere of radius r which intercepts a beam of molecules with uniform speed V_∞ as shown in Fig. 13. Expressing the force exerted on a toroidal differential area dA as a function of the average normal and tangential momentum accommodation coefficients (functions of θ_i) and summing over the upper half area of the sphere, one obtains

$$\sum \frac{\text{no. of collisions}}{\text{time x area}} \; dA \left[(p_i - p_w)_N (\alpha_{NM} \cos\theta_i) + (p_i - p_w)_T (\alpha_{TM} \sin\theta_i) \right] = \frac{1}{2} C_D \, nm \, V_\infty^2 \, A$$

The number of collisions per unit area per unit time is nV_∞; the differential area is

$$dA = 2\pi r \sin\theta_i (r d\theta_i) \cos\theta_i = 2\pi r^2 \sin\theta_i \cos\theta_i d\theta_i$$

Then

$$\sum nV_\infty 2\pi r^2 \sin\theta_i d\theta_i \left[(p_i - p_w)_N (\alpha_{NM} \cos\theta_i) + (p_i - p_w)_T (\alpha_{TM} \sin\theta_i) \right] \cos\theta_i = \frac{1}{2} C_D \, nm \, V_\infty^2 A$$

which may be simplified to

$$2\pi \, V_\infty r^2 \sum \left[(p_i - p_w)_N (\alpha_{NM} \cos\theta_i) + (p_i - p_w)_T (\alpha_{TM} \sin\theta_i) \right] \sin\theta_i \cos\theta_i d\theta_i = \frac{1}{2} C_D \, m \, V_\infty^2 A$$

Since $A = \pi r^2$ and $p = mV$, the drag coefficient C_D may be written

$$C_D = \frac{4}{V_\infty} \sum_{\theta_i = 0}^{\pi/2} \left[(V_\infty - V_w)_N \alpha_{NM} \cos\theta_i + (V_\infty - V_w)_T \alpha_{TM} \sin\theta_i \right] x \, \sin\theta_i \cos\theta_i d\theta_i$$

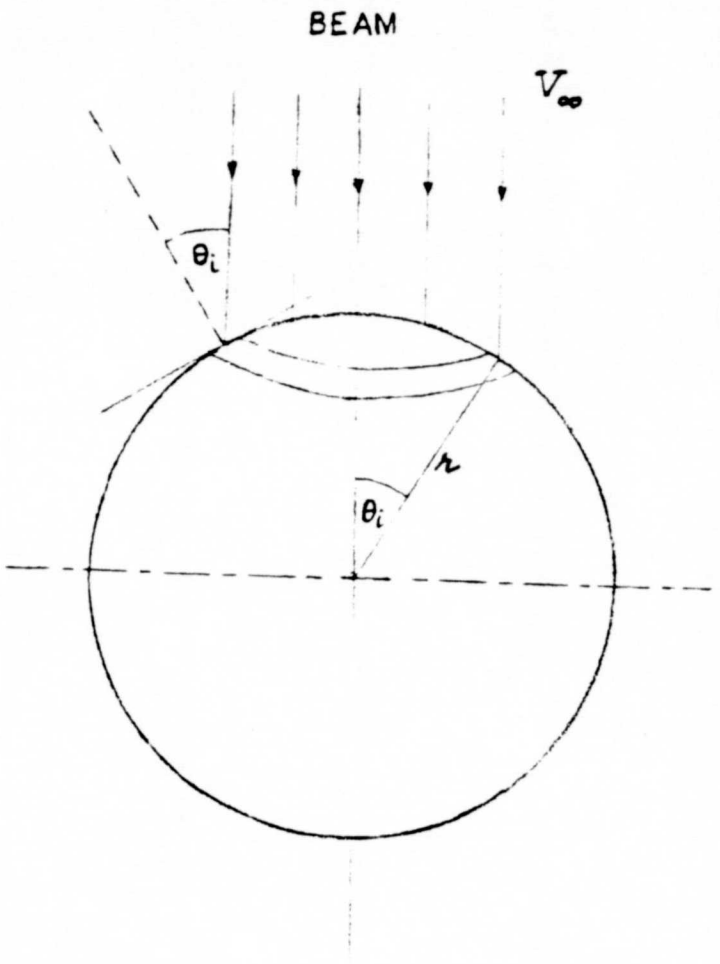

FIG.13 REPRESENTATION OF A SPHERE MOVING IN A RAREFIED ATMOSPHERE

For the co-ordinate system shown in Fig. 10,

$$V_{\infty_N} = V_\infty \cos\theta_i$$

$$V_{\infty_T} = V_\infty \sin\theta_i$$

$$V_{w_N} = \left[\frac{\pi}{2} \frac{kT}{m} \right]^{1/2}$$

$$V_{w_T} = o$$

The latter five equations were used in the evaluation of the drag coefficient given in Chapter IV of this report.

ORIGINAL PAGE IS
OF POOR QUALITY

APPENDIX B

Computer Program for Evaluation of C_D for a Sphere

(latest)

```
      *JOB                                                                  WSY00160
      C     CALCULATION OF DRAG COEFFICIENT FOR SPHERES                     WSY00180
    1       VI=7000.0                                                       WSY00200
    2       N=0                                                             WSY00220
    3       DEL=1.570796/1000                                               WSY00240
    4       U=7000.0                                                        WSY00260
    5       THETAI=-DEL                                                     WSY00280
    6       SUM=0.0                                                         WSY00300
    7       WRITE(6,15)                                                     WSY00320
    8   15  FORMAT(6X,1HN,6X,6HTHETAI,5X,2HCD)                              WSY00340
    9   20  THETAI=THETAI+DEL                                               WSY00360
   10       N=N+1                                                           WSY00380
   11       ACNM=1.28+0.178*THETAI                                          WSY00400
   12       ACTM=1.00                                                       WSY00420
   13       VIN=VI*COS(THETAI)                                              WSY00440
   14       VIT=VI*SIN(THETAI)                                              WSY00460
   15       VWN=-1363.0+0.707                                               WSY00480
   16       SUM=SUM+((VIN-VWN)*ACNM*COS(THETAI)+VIT*ACTM*SIN(THETAI))       WSY00500
     A        *SIN(THETAI)*COS(THETAI)*DEL                                  WSY00520
   17       IF (THETAI-1.57078) 20,40,40                                    WSY00540
   18   40  CD=SUM*4.0/U                                                    WSY00560
   19       WRITE (6,50) N,THETAI,CD                                        WSY00580
   20   50  FORMAT(6X,I4,3X,F7.4,4X,E11.4)                                  WSY00600
   21       STOP                                                            WSY00620
   22       END                                                             WSY00640

      *RUN                                                                  WSY00660
    N      THETAI      CD
 1002      1.5723      0.2641E 01

CORE USAGE        OBJECT CODE=     1040 BYTES,ARRAY AREA=        0 BYTES,TOTAL AREA AVAILABLE=    53248  BYTES

DIAGNOSTICS         NUMBER OF ERRORS=        0, NUMBER OF WARNINGS=        0, NUMBER OF EXTENSIONS=        0

COMPILE TIME=      0.02 SEC,EXECUTION TIME=      0.32 SEC,  WATFIV - JUL 1973 V1L4       14.08.19     THURSDA

      *WATEND                                                               WSY00680
```